Quaternary Research

doi:10.1017/qua.2019.69

Crustal subsidence inferred from reconstruction of the Pleistocene–Holocene palaeogeography in the northern Lake Inba area, central Japan

Takashi Chiba[a]*, Shigeo Sugihara[b], Yoshiaki Matsushima[c], Yusuke Arai[d], Kunihiko Endo[e]

[a]Faculty of Bioresource Sciences, Akita Prefectural University, 241–438 Kaidobata-Nishi, Nakano, Shimoshinjo, Akita-shi, Akita 010-0195, Japan
[b]Meiji University, 1–1 Kanda-Surugadai, Chiyoda-ku, Tokyo, 101–8301 Japan
[c]Kanagawa Prefectural Museum of Natural History, 499 Iryuda, Odawara-shi, Kanagawa, 250-0031, Japan
[d]Environmental Planning Bureau, City of Yokohama, Kannai Chuou Building, 2–22 Masagocho, Naka-ku, Yokohama-shi, Kanagawa, 231-0016, Japan
[e]Nihon University, 3-25-40 Sakurajosui, Setagaya-Ku, Tokyo, 156-8550, Japan
*Corresponding author e-mail address: chibat@akita-pu.ac.jp (T. Chiba).

(Received April 13, 2019; Accepted September 30, 2019)

ABSTRACT

To help characterise the palaeogeographic and lacustrine environmental changes that resulted from the Holocene transgression and residual subsidence in the eastern Kanto Plain of central Japan, we analysed four drill cores and reviewed other core data from the southern part of the Lake Inba area. Fossil diatom assemblages yielded evidence of centennial-scale palaeogeographic and salinity responses to sea-level changes since the late Pleistocene. We determined that the seawater incursion into the Lake Inba area during the Holocene transgression occurred at approximately 9000 yr. We also recognised a late Holocene regression event corresponding to the Yayoi regression, considered to have occurred from ca. 3000 to ca. 2000 yr, and a subsequent transgression. Our data clarify some of the palaeogeographic changes that occurred in the Lake Inba area and document an overall trend toward lower salinity in the lake during the regression. In particular, the environment in Lake Inba changed from brackish to freshwater no later than 1000 yr. From the detailed palaeogeographic and palaeo-sea-level reconstruction, we recognised that residual subsidence occurred during the Holocene in this area. Thus, comparison of sea-level reconstructions based on modelling and fossil diatom assemblages is effective in interpreting Holocene long-term subsidence.

Keywords: Late Pleistocene; Holocene; Diatom; Sea-level change; Palaeogeography; Tectonic subsidence; Lake Inba; Japan

INTRODUCTION

The study of sea-level changes from the late Pleistocene to the Holocene is among the most important research areas in Quaternary studies (Clark et al., 1978; Shennan, 1982; Nakada and Lambeck, 1989; Yokoyama et al., 2012; Okuno et al., 2014; Lambeck et al., 2014; Khan et al., 2015; García-Artola et al., 2018; Horton et al., 2018; Vacchi et al., 2018) because the cycle of eustatic sea-level changes has been more clearly recognised during the Quaternary period than prior (Lisiecki and Raymo, 2005; Naish and Wilson, 2009).

Holocene relative sea-level changes exhibit spatial and temporal variability that arises mainly from the interaction of eustatic and isostatic factors (Clark et al., 1978; Khan et al., 2015). The records of Holocene relative sea-level changes in far-fields exhibit a mid-Holocene high stand, the timing (between 8 and 4 ka) and magnitude (between <1 and 6 m) of which vary among South America, Africa, Asia, and Oceania regions (Khan et al., 2015). However, it is difficult to obtain quantitative sea-level data from tectonically active zones such as subduction zones. The coastal lowland of Japan is within such a zone (Fig. 1a); thus, relative sea-level changes reconstructed from late Quaternary sedimentary deposits incorporate tectonic effects (Yokoyama et al., 1996, 2012; Sato et al., 2001; Tanabe et al., 2009; Tanigawa et al., 2013). In other words, through a detailed reconstruction of the palaeogeography and local tectonic effects after separating both, we may be able to better understand both sea-level changes and tectonics.

Cite this article: Chiba, T., Sugihara, S., Matsushima, Y., Arai, Y., Endo, K. 2020. Crustal subsidence inferred from reconstruction of the Pleistocene–Holocene palaeogeography in the northern Lake Inba area, central Japan. *Quaternary Research* 94, 61–79. https://doi.org/10.1017/qua.2019.69

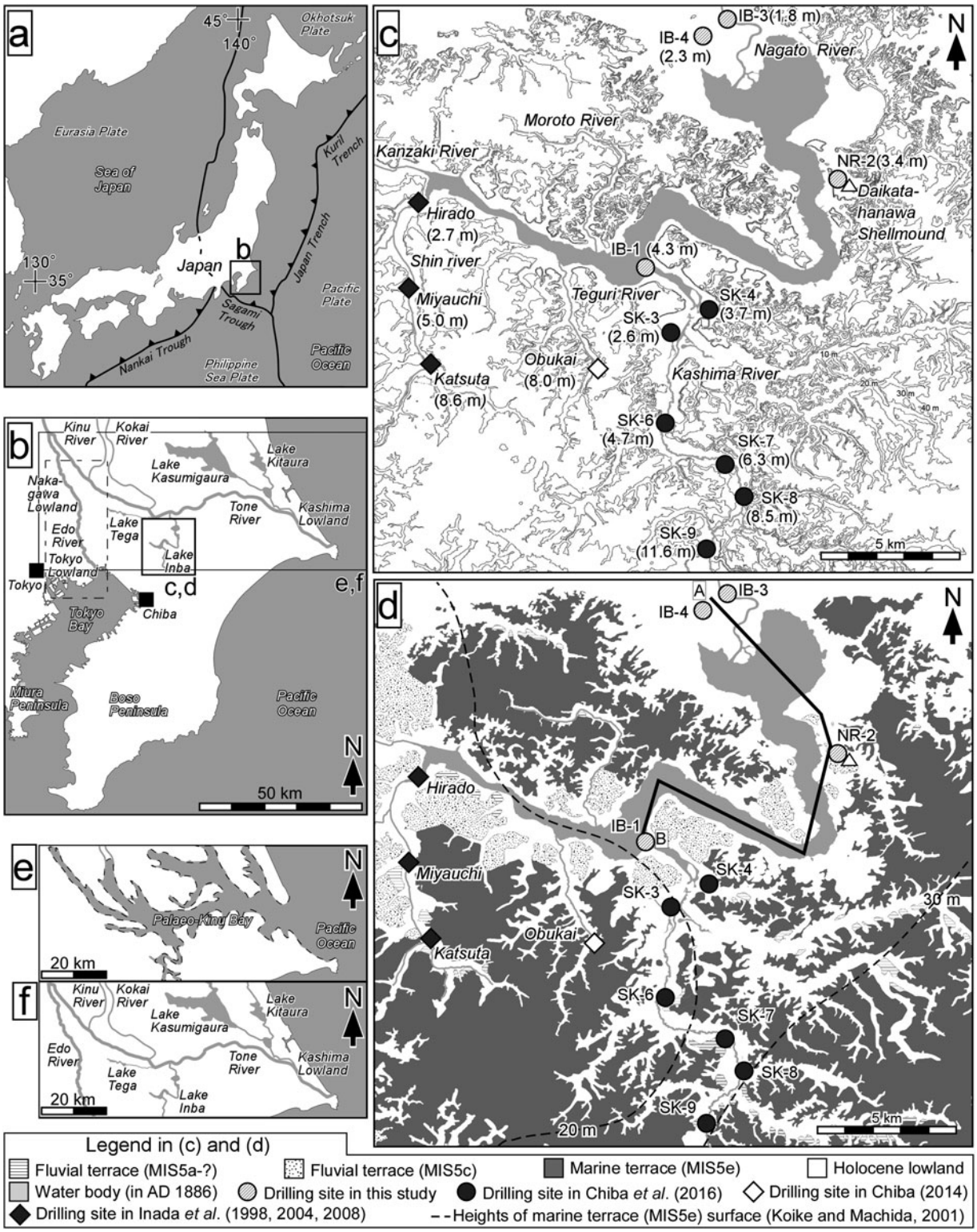

Figure 1. Maps showing: (a) the location of the study area in Japan; (b) the Kanto Plain; and drilling sites described in (c) the studies of Chiba et al. (2016; SK-3–SK-9) and Inada et al. (1998, 2004, 2008; Hirado, Miyauchi, and Katsuta) and (d) this study (IB-1, 3, 4, and NR-2). The contour interval in (c) is 10 m (Tani 2015, 2016) and the lake shoreline is based on the Jinsokuzu map created in AD 1886 (Iwasaki et al., 2009; National Institute for Agro-Environmental Sciences 2016). The map in (d) shows the geographic setting of the study area (modified from Sugihara, 1970; Sugihara et al., 2011) and contours representing the height of a marine terrace formed during Marine Oxygen Isotope Stage 5e (Koike and Machida 2001). (e) Map showing the water body area during the Holocene transgression period based on Endo et al. (1983). (f) The modern water body area.

https://doi.org/10.1017/qua.2019.69 Published online by Cambridge University Press

On the eastern Kanto Plain of central Japan (Fig. 1a and b), the vast lowland along the Tone River has yielded evidence of landform development and palaeoenvironmental changes caused by the Holocene transgression and the subsequent regression (Kikuchi, 1969; Ota et al., 1985; Saito, 1995; Saito et al., 2016). During the Holocene transgression, the present-day lowlands along the middle and lower reaches of the Tone River (Fig. 1b) were covered by a shallow bay (Endo et al., 1982, 1983), whereas during the subsequent regression, the area was characterised by lagoons and drowned valleys filled with marine mud. Moreover, during the Holocene, prehistoric human inhabitants (the Jomon culture during the early to late Holocene and the Yayoi culture during the late Holocene) left behind many shell mounds near contemporary shorelines (Yoshino, 1998; Editorial Committee of History in Noda-shi, 2010; Masubuchi and Sugihara, 2010). The relationship between the palaeoenvironment and human activity have been actively studied (e.g., Masubuchi and Sugihara, 2010). Evidence of Holocene sea-level change is abundant on the eastern Kanto Plain (Endo et al., 1982; Ota et al., 1990; Chiba et al., 2016). The topography of the southern Kanto Plain has also been strongly influenced by Quaternary tectonics (Sugimura and Naruse, 1954; Yonekura, 1975; Matsuda et al., 1978; Nakata et al., 1980; Kaizuka, 1987; Shishikura, 2003, 2014; Hashima et al., 2016; Noda et al., 2018); for example, the present height of the deposits associated with the Holocene high stand increases toward the southern Kanto. Therefore, to understand the formational processes of the geomorphic history in the Kanto area, it is necessary to reconstruct palaeogeographic changes resulting from both sea-level changes and tectonics.

Despite the importance of tectonics, the magnitude and timing of tectonic movements of the central to eastern Kanto Plain at a millennial scale are poorly understood mainly for two reasons (Kaizuka et al., 2000). First, the central to northern Kanto Plain has been subsiding (Kaizuka et al., 2000) and the pre-Holocene sediments and erosional topography formed during the last glacial maximum are covered by thick, marine sediments deposited during the Holocene transgression whereas the southern Kanto Plain underwent uplift. Second, the coastal environment and landforms have been greatly altered by human activities (Kaizuka et al., 2000).

However, a long, narrow, inner bay, the so-called Palaeo-Kinu Bay (or Sea of Katori), formed in the eastern Kanto area during the transgression period (Fig. 1e; Endo et al., 1983; Komatsubara et al., 2017). The bay existed for a long time before disappearing (Fig. 1f), although it is estimated that the Palaeo-Kinu Bay contracted and desalinated during the regression. One theory states that the water body area remained until the fourteenth century (Oya, 1969); however, the details remain unknown. Chiba et al. (2016) analysed the diatomaceous record in cores (SK-3 and -4 and SK-6–9) collected at sites along the Kashima River south of Lake Inba and estimated the palaeotidal range at 7000 yr, inferred sea-level changes and the timing and height of the Holocene high stand, and estimated the effect of residual uplift during the last 8000 yr (Fig. 1c). The estimated uplift trend is consistent with the model of Okuno et al. (2014). The crustal uplift trend over ~125,000 yr in the Kanto region suggests that tectonic movements have been approximately consistent during the past ~125,000 yr. Moreover, the uplift trend can be explained by crustal deformation owing to subduction of the Philippine Sea plate beneath the Kanto region (Fig. 1a and b; Hashima et al., 2016; Noda et al., 2018). However, the area south of Lake Inba (including along the Kashima River) is tectonically active; thus, the standard sea-level curve is not necessarily applicable. Moreover, it is possible that the mode of vertical crustal movement varies between the southern and northern parts of the Lake Inba area. The present heights of the marine terraces (Koike and Machida, 2001) suggest that the residual uplift rate differs between the upland area south of the lake and the low-elevation area around its outlet (Fig. 1d).

To assess in detail the effects of tectonics on the eastern Kanto Plain during the latest Pleistocene, we obtained four drill cores from the central and northern Lake Inba area and reconstructed the palaeogeography and relative sea-level changes by means of fossil diatom analysis and ^{14}C dating. Using these data together with diatomaceous and ^{14}C data from Obukai, an upland site south of Lake Inba (Fig. 1c and d; Chiba, 2014), we compared the rate of sea-level rise to that of the relative sea-level model calculated by Okuno et al. (2014). We also compared the rate of sea-level rise to that of the Tokyo and Nakagawa lowlands (Fig. 1b, Endo et al., 1989; Ishihara et al., 2012; Tanabe et al., 2015; Tanabe, 2019), where the effect of crustal deformation during the Holocene is considered to have been small (Endo et al., 1989; Tanabe, 2019).

GEOLOGICAL SETTING

The lowlands along the lower reaches of the Tone River are covered by Holocene sediments (Endo et al., 1983; Sugihara et al., 2011), but the distribution of marine and fluvial terraces at 20–30 m elevation, dating from Marine Oxygen Isotope Stage (MIS) 5a–5e, attests to gradual uplift occurring during the late Pleistocene and Holocene (Sugihara, 1970; Kaizuka, 1987). In addition, Holocene sea-level changes have influenced the topography of the eastern Kanto Plain (Kaizuka et al., 2000). During the Holocene transgression, many stream valleys that were incised during the last glacial period became filled by marine sediments, and coastal landforms were formed (Endo et al., 1983). During the sea-level high stand, fluvial deposits blanketed the marine sediments, and lagoons formed that became lake basins following the ensuing regression. For example, Lake Kasumigaura (Saito et al., 1990), Lake Kitaura (Naya et al., 2007), and Lake Tega (Kashima et al., 1988) are former lagoons (Fig. 1b). Lake Inba, another former lagoon (Kusuda and Nirei, 1994; Sugihara et al., 2011), has been divided by land reclamation into northeastern and southwestern parts. At present, its surface area is 11.55 km^2, its average depth is 1.7 m, and its maximum

https://doi.org/10.1017/qua.2019.69 Published online by Cambridge University Press

depth is 2.5 m (Chiba Prefectural Environmental Research Center, 2016). The Kashima, Shin, Kanzaki, Moroto, and Teguri rivers flow into Lake Inba, and the lake drains from its north end into the Tone River (Fig. 1c and d). The present elevation of the lowlands around the lakeshore is ~12 m, and this lowland area is underlain by about 10–40 m of Holocene deposits (Sugihara et al., 2011). From AD 1946–1968, reclamation works were carried out around Lake Inba (Takada et al., 1971), and most of the reclaimed lands are now used for farming.

MATERIALS AND METHODS

Lithology and dating

We used samples collected from cores IB-3 and -4 (Fig. 1d and 2), which were obtained near where Lake Inba connects with the Tone River, from core NR-2 (Fig. 1d and 2), which was collected near the Daikatahanawa shell mound (Chiba et al., 2011), and from core IB-1, which was obtained near where the Kashima River flows into Lake Inba (Fig. 1d and 2). Lithological characteristics of the cores were described, based on changes in grain size and colour of sediments, content, and conservation of biogenic material such as fossil shells and plants. The cores were subsampled first for ^{14}C dating (Sugihara et al., 2011) and later by us to obtain samples for diatom and grain-size analyses. We used the ^{14}C age data reported by Sugihara et al. (2011) along with new ^{14}C date obtained from IB-3 and -4 (Table 1). All dates were calibrated by using the database of Reimer et al. (2004) and the IntCal 6.0 program, and calendar ages and their 2-sigma range (cal yr BP) are used here. For dates obtained on marine materials such as shell, we assumed a value of 0 for the reservoir effect, ΔR (the difference between regional and global marine ^{14}C ages; Stuiver and Braziunas, 1993), because the correct value for this area is unknown.

Sand content

To assist observation of the core lithology, we measured sand content (%). The samples were collected from cores IB-1, -3, and -4 and NR-2 at 0.1- to 0.5-m intervals (88 samples from IB-3, 50 samples from IB-4, 20 samples from NR-2, and 52 samples from IB-1). The samples were pretreated with H_2O_2 and plant materials such as wood fragments were picked out. After the pretreatment, samples were divided into mud and sand by sieving through a 4-phi (0.063-mm) mesh.

Diatom analysis

Samples for diatom analysis were collected from cores IB-1, -3, and -4 at 0.1- to 1.0-m intervals (52 samples from IB-3, 32 samples from IB-4, and 38 samples from IB-1). Diatoms of core NR-2 have been reported by Chiba et al. (2011), so we also collected and analysed eight samples from core NR-2 and added the results to the reported data. The samples were pretreated with H_2O_2, and then the cleaned diatom frustules were mounted in Pleurax. Relative abundances of diatom species were determined by counting at least 300 valves under an optical microscope at 1000× using oil immersion. Diatom identifications were made and environmental conditions were interpreted by reference to Hasle (1978), Krammer and Lange-Bertalot (1986, 1988, 1991a, 1991b), Krammer (2000), Witkowski et al. (2000), Sawai (2001), Nagumo (2003), Sawai and Nagumo (2003), Idei et al. (2012), Watanabe et al. (2013), Chiba and Sawai (2014), Chiba et al. (2018), and Cocquyt et al. (2018).

Reconstruction of palaeoshorelines and sea-level changes

To reconstruct palaeoshoreline changes, we used diatom analysis results from cores IB-1, -3, and -4 and NR-2, along with previously reported results from Obukai (Chiba 2014) and cores SK-3–SK-9 (Fig. 1c and d; Chiba et al., 2016). We also used palaeoenvironmental changes along the Shin River, which flows into the western end of Lake Inba, reported by Inada et al. (1998, 2004, 2008), in our reconstruction. In general, we used tidal flat sediments, which we identified by an abundance of diatom species considered to be tidal flat indicators (Chiba and Sawai, 2014; Chiba et al., 2016) as a palaeoshoreline indicator, because tidal flats are typically in intertidal areas (at around mean sea level). These sea-level index points, however, have an error equal to the palaeotidal range. *Pseudopodosira kosugii* is a useful indicator diatom species for the upper limit of marine deposits (Tanimura and Sato, 1997; Sawai, 2001), but this species is not always abundant in Holocene sediments in the northern part of the study area. Therefore, we determined the high-tide level (the upper limit of the tidal range) from the upper limit of the low-salinity diatom assemblage, which is typically found just below the upper marine limit, and the core lithology (in particular, the presence of peaty deposits). Where we could identify the high-tide level near the marine limit, we considered the tidal range to be 3.3 m (Chiba et al., 2016); otherwise, we assumed a tidal range of 6.6 m where we were unable to determine the upper and lower limits of the tidal range. We also used changes in the diatom assemblage type (freshwater, freshwater-brackish to brackish-marine, and marine) to identify changes in the depositional environment (Appendices 1–3).

Estimation of the subsidence rate

The mean subsidence rate was calculated from the amount of subsidence divided by the amount of time over which the subsidence occurred; this information was derived from the elevations and ages of each sea-level index point obtained by dating and diatom analysis in this study or simulated values from prior studies (e.g., Okuno et al., 2014). The mean subsidence rate was calculated from the following equation:

$$\text{mean subsidence rate} = \frac{E_1 - E_2}{T}$$

https://doi.org/10.1017/qua.2019.69 Published online by Cambridge University Press

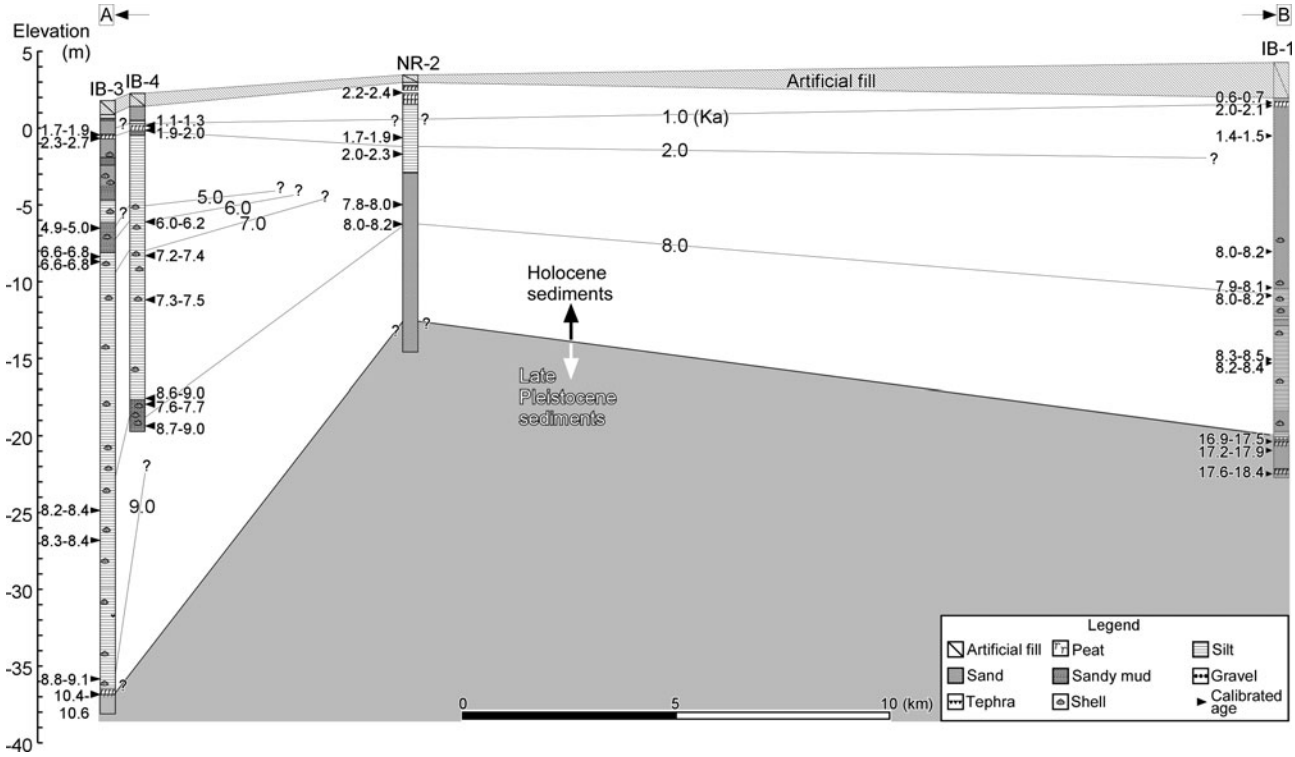

Figure 2. Cross section along line A–B in Figure 1d.

where E_1 is the elevation of a sea-level index point or a simulated value, E_2 is the elevation of a sea-level index point or a simulated value, and T is the time period for which the subsidence was estimated by palaeoenvironmental reconstruction.

RESULTS

Palaeoenvironments inferred from the lithology and diatom assemblages of IB-3

Core IB-3 contained Holocene deposits (Fig. 3). The interval from 39.0–38.5 m consisted of peaty sediments (sand content 30–68%) overlying fine to medium sand from 40.0–39.0 m depth (sand content 65–79%). The sediments of the upper sandy muddy deposits consisted of sandy mud from 38.5–37.9 m depth; the interval from 38.5–37.9 m depth consisted of sandy mud (sand content 6–52%). The interval from 37.9–10.0 m depth consisted of mud, containing fossil shells, and that from 8.0–5.2 m depth also contained shell fragments (sand content 8–59%). The interval from 2.6–2.2 m depth consisted of peat and that from 4.1–3.8 m depth consisted of organic-rich muddy sand and a 1.2-m-thick coarse sand bed overlying a lower mud with an erosional contact (sand content 31–58%). An organic-rich sandy mud from 2.2–1.9 m depth with an erosional contact (sand content 2–24%) underlies an upward-fining sequence from medium to fine sand from 1.9–1.1 m depth. The natural sediments consisted of muddy sand from 1.1–0.9 m in depth; below the artificial fill occupied the uppermost 0.9 m.

In core IB-3, we identified diatom zones 1 to 5 in ascending order (Fig. 3). Zone 1 was characterised by freshwater diatoms such as *Eunotia* spp. and *Planothidium lanceolatum* and mainly sandy sediments; thus, it was interpreted as representing a freshwater environment. In diatom zone 2, freshwater diatoms decreased and freshwater-brackish, brackish-marine, and marine diatoms such as *Amphora arenicola* and *Diploneis smithii* increased in relative abundance. Lithologically, this zone was characterised by peat or organic-rich mud. Given the mixed diatom assemblage and lithology, this zone was interpreted as representing a muddy tidal flat environment. In diatom zone 3, marine planktonic diatoms such as *Cyclotella litoralis* and *Thalassionema nitzschioides* dominated and the lithology was very fine mud; therefore, this zone was interpreted as representing a subtidal inner bay environment. In zone 4, freshwater diatoms such as *Staurosira construens* and freshwater-brackish diatoms such as *Pseudostaurosira brevistriata* and *Pseudostaurosira* sp. increased; furthermore, the intertidal diatom *Terpsinoë americana* was recognised. Given the diatom assemblage and the mud or sandy mud lithology, this deposit was interpreted as representing a brackish water environment such as tidal flats. In zone 5, the relative abundance of brackish-marine species decreased to near zero, and freshwater-brackish species such as *P. brevistriata* and freshwater species such as *S. construens* increased. Lithologically, this zone consisted of sandy or peaty deposits. Therefore, zone 5 was interpreted as representing a freshwater or low-salinity marsh environment with a fluvial influence.

https://doi.org/10.1017/qua.2019.69 Published online by Cambridge University Press

Table 1. List of ^{14}C ages in this study. All elevations and calibrated dates are rounded to the nearest 10 cm and 10 yr, respectively. Tidal range showing sea-level index points; F, freshwater environment (non-tidal wetland); UIT, just below the marine limit and upper intertidal zone; IT, intertidal zone, ST, subtidal zone

Lab. Cord	Site	Depth (m)	Elevation (m)	Material	Method	$\delta^{13}C$ (‰)	^{14}C (yr BP ± 1σ)	cal yr BP (1σ)	cal yr BP (2σ)	Environment	Tidal range
IAAA-90670	IB-3	2.3	−0.5	Peat (Bulk)	AMS	−26±0.4	1840±30	1740–1820	1710–1870	Salt marsh	UIT
IAAA-90671	IB-3	2.6	−0.8	Organic mud (Bulk)	AMS	−23±0.4	2380±30	2350–2370 2390–2400 2410–2460	2340–2660	Tidal flat	IT
IAAA-90672	IB-3	8.5	−6.7	Organic mud (Bulk)	AMS	−19±0.4	4370±40	4870–4970	4850–5040	Inner bay	ST
IAAA-90673	IB-3	10.5	−8.7	Shell	AMS	−3±0.5	6270±40	6670–6770	6620–6840	Inner bay	ST
IAAA-90674	IB-3	10.8	−9	Shell	AMS	−1±0.4	6250±40	6650–6750	6600–6820	Inner bay	ST
Beta-462977	IB-4	26.5	−24.7	Shell	AMS	−0.8	7850±30	8300–8360	8230–8390	Inner bay	ST
Beta-462218	IB-3	29.5	−26.7	Shell	AMS	−0.8	7860±30	8310–8370	8250–8400	Inner bay	ST
IAAA-90675	IB-3	38.1	−36.3	Shell	AMS	0.5±0.5	8360±50	8860–9020	8750–9090	Tidal flat	IT
IAAA-90676	IB-3	38.9	−37.1	Peat (Bulk)	AMS	−27±0.6	9670±50	10,490–10,580	10,410–10,630	Freshwater environment	F
Beta-432319	IB-4	2.2	0.1	Seed	AMS	−24.9	1230±30	1090–1110 1120–1160 1170–1180 1210–1240	1070–1260	Freshwater environment	F
IAAA-90677	IB-4	2.4	−0.1	Peat (Bulk)	AMS	−28±0.3	2000±30	1900–1910 1920–1990	1880–2040	Salt marsh	UIT
IAAA-90678	IB-4	8.4	−6.1	Shell	AMS	−2.9±0.4	5680±40	7250–7350	5970–6200	Inner bay	ST
IAAA-90679	IB-4	10.5	−8.2	Shell	AMS	−0.7±0.4	6770±40	7250–7350	7220–7400	Inner bay	ST
IAAA-90680	IB-4	13.1	−10.8	Shell	AMS	−0.2±0.4	6920±40	7400–7470	7330–7510	Inner bay	ST
IAAA-90681	IB-4	19.9	−17.6	Shell	AMS	−4.2±0.4	8330±40	8850–8990	8740–9010	Inner bay	ST
Beta-484171	IB-4	20.2	−17.9	Shell	AMS	−0.8	7150±30	7580–7650	7560–7680	Inner bay	ST
IAAA-90682	IB-4	21.6	−19.3	Shell	AMS	−1.6±0.4	8640±40	9270–9390	9190–9430	Inner bay	ST
Tka-14730	NR-2	1.2	2.2	Peat (Bulk)	AMS	−20.9	2280±30	2190–2190 2270–2230 2310–2350	2160–2350	Salt marsh	UIT
Tka-14731	NR-2	4.2	−0.8	Plant	AMS	−26	1850±30	1740–1820	1710–1870	Tidal flat	IT
Tka-14732	NR-2	5.2	−1.8	Plant	AMS	−26.1	2100±40	2010–2120 2040–2120	1950–2300	Inner bay	ST
Tka-14733	NR-2	8.4	−5	Shell	AMS	0.6	7470±40	7880–7890 7840–7980	7840–8010	Inner bay	ST
Tka-14734	NR-2	9.7	−6.3	Shell	AMS	−2.7	7600±40	8000–8110	7960–8160	Inner bay	ST
IAAA-90644	IB-1	2.6	1.7	Peat (Bulk)	AMS	−23±0.4	780±30	680–700 700–710 720–730	670–740	Freshwater environment	F
IAAA-90645	IB-1	2.9	1.4	Peat (Bulk)	AMS	−28±0.5	2090±30	2000–2030 2040–2070 2080–2110	1990–2140	Salt marsh	UIT
IAAA-90646	IB-1	4.8	−0.5	Plant	AMS	−26±0.4	1560±30		1390–1530	Tidal flat	IT

							1410–1420				
							1430–1440				
							1460–1520				
IAAA-90647	IB-1	12.7	−8.4	Shell	AMS	−3±0.5	7590±40	7990–8100	7960–8150	Inner bay	ST
IAAA-90648	IB-1	14.7	−10.4	Shell	AMS	−1±0.4	7530±40	7940–8020	7910–8110	Inner bay	ST
IAAA-90649	IB-1	15.2	−10.9	Shell	AMS	−0.9±0.6	7630±40	8040–8140	7990–8180	Inner bay	ST
IAAA-90650	IB-1	19.3	−15	Shell	AMS	−2.1±0.5	7910±40	8330–8410	8290–8470	Inner bay	ST
IAAA-90651	IB-1	19.5	−15.2	Wood	AMS	−28±0.4	7460±40	8210–8260	8190–8370	Inner bay	ST
								8290–8340			
IAAA-90652	IB-1	24.7	−20.4	Peat (Bulk)	AMS	−29±0.5	14090±60	16,940–17,240	16,890–17,480	Freshwater environment	F
IAAA-90653	IB-1	25.3	−21	Wood	AMS	−26±0.7	14470±60	17,480–17,830	17,230–17,900	Freshwater environment	F
IAAA-90654	IB-1	26.8	−22.5	Wood	AMS	−28±0.4	14720±60	17,750–18,020	18,300–18,450	Freshwater environment	F
								17,620–18,070			

The tidal flat environment suggested by the lithologic and diatomaceous data of zone 2 indicates that mean sea level during the period 9090–8750 cal yr BP was at approximately 38.1 m core depth (elevation −36.3 m). A subtidal environment prevailed at the site from approximately 8750 to 4850 cal yr BP (8.5 m core depth; elevation −6.7 m). However, by 2660 cal yr BP (2.6 m core depth; elevation −0.8 m), the environment at the site was again tidal flats and thus was near mean sea level. During the period 1870–1710 cal yr BP, the site was characterised by a low-salinity environment (2.3–2.6 m core depth; elevation −0.5 to −0.8 m).

Palaeoenvironments inferred from the lithology and diatom assemblages of IB-4

Core IB-4 contained sandy mud with shell fragments extending from 22.0–20.4 m depth (sand content 34–66%) and mud containing shells and shell fragments extending from 20.4–3.0 m depth (sand content 2–41%). Upward-fining sandy mud deposits were found from 3.0–2.6 m depth (sand content 66–88%). The interval from 2.5–2.0 m depth consisted of peat; fine sand with reverse grading was found from 2.6–2.5 m depth (sand content 1–13%). The sand deposits overlie organic-rich, peaty mud from 2.0–1.8 m depth with an erosional contact (sand content 9–40%). The interval from 1.4–1.0 m depth was characterised by mud sand and that from 1.8–1.4 m depth by fine to coarse sand (sand content 93–98%). The sediments from 1.0–0.9 m depth consisted of fine and medium sand with normal grading in the upper part and reverse grading in the lower part (sand content 95%); artificial fill was found from 0.9 m depth to the surface.

In core IB-4, we identified diatom zones 1 to 5 in ascending order (Fig. 4). Zone 1 was characterised by marine and brackish-marine diatoms such as *Thalassionema nitzschioides*, *Thalassiosira* spp., and *Cyclotella litoralis* and lithologically mainly consisted of sandy mud or mud. Thus, zone 1 was interpreted as representing a marine environment. In diatom zone 2, marine planktonic diatoms decreased and brackish-marine diatoms such as *Diploneis smithii*, *Planothidium delicatulum*, and *Petroneis marina* increased. Freshwater-brackish species such as *Pseudostaurosira brevistriata* also increased. Lithologically, the zone was characterised by mud and poorly sorted sand. Therefore, zone 2 represents a tidal flat environment. Zone 3 was characterised by the freshwater and freshwater-brackish species *Staurosira construens*, *Pseudostaurosira brevistriata*, *Pseudostaurosira subsalina*, *Pseudostaurosira* sp., and, in peat, *Pinnunavis elegans*. Thus, zone 3 represents a salt marsh environment. In diatom zone 4, marine diatoms disappeared and freshwater-brackish species and freshwater species increased. Therefore, zone 4 represents a freshwater marsh environment. Zone 5 was characterised by freshwater diatoms such as *Staurosira construens*, *Ulnaria ulna*, and *Cocconeis placentula* and a sandy lithology. Thus, it represents a freshwater environment.

https://doi.org/10.1017/qua.2019.69 Published online by Cambridge University Press

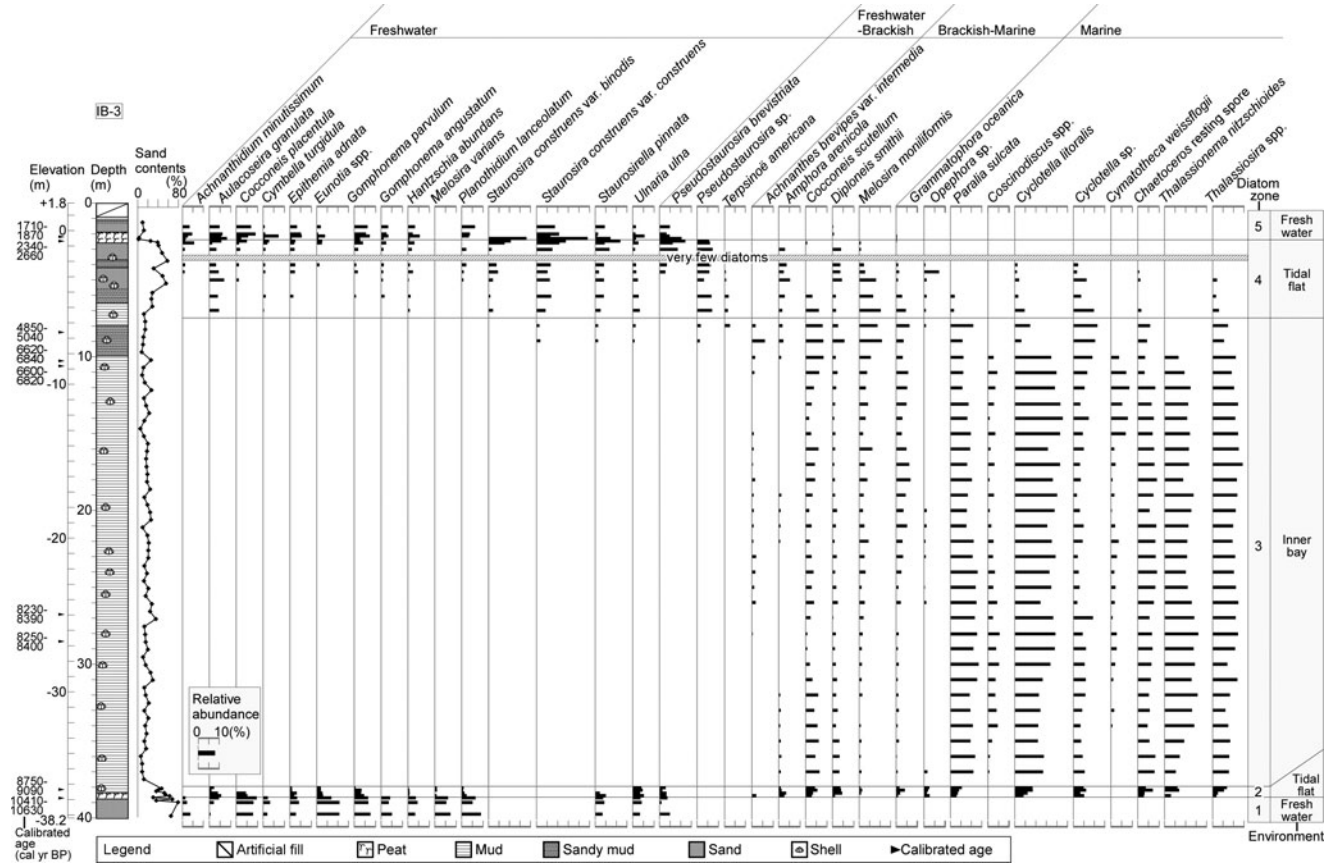

Figure 3. Stratigraphy, diatom assemblages, and ^{14}C ages in core IB-3.

The lithologic and diatomaceous data suggest that mean sea level at approximately 9000 cal yr BP was at 22.0 m core depth (elevation −19.7 m), though there is a high probability that the ^{14}C-dated materials from 19.9 m and 21.6 m depth were reworked because they consisted of shell fragments. A subtidal environment prevailed at the core site from 7510 cal yr BP until at least 5970 cal yr BP. Subsequently, a tidal flat environment formed, but its duration is unknown because of a lack of dated samples. The high-tide level during the period 2030–1880 cal yr BP was at 2.4–

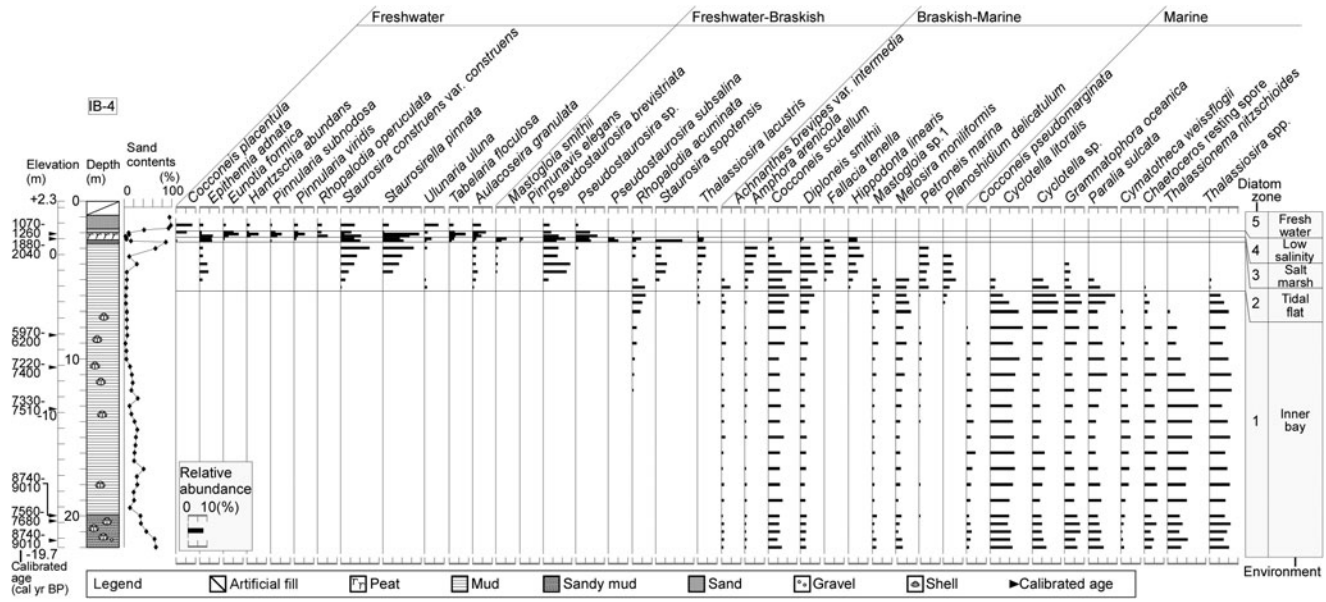

Figure 4. Stratigraphy, diatom assemblages, and ^{14}C ages in core IB-4.

https://doi.org/10.1017/qua.2019.69 Published online by Cambridge University Press

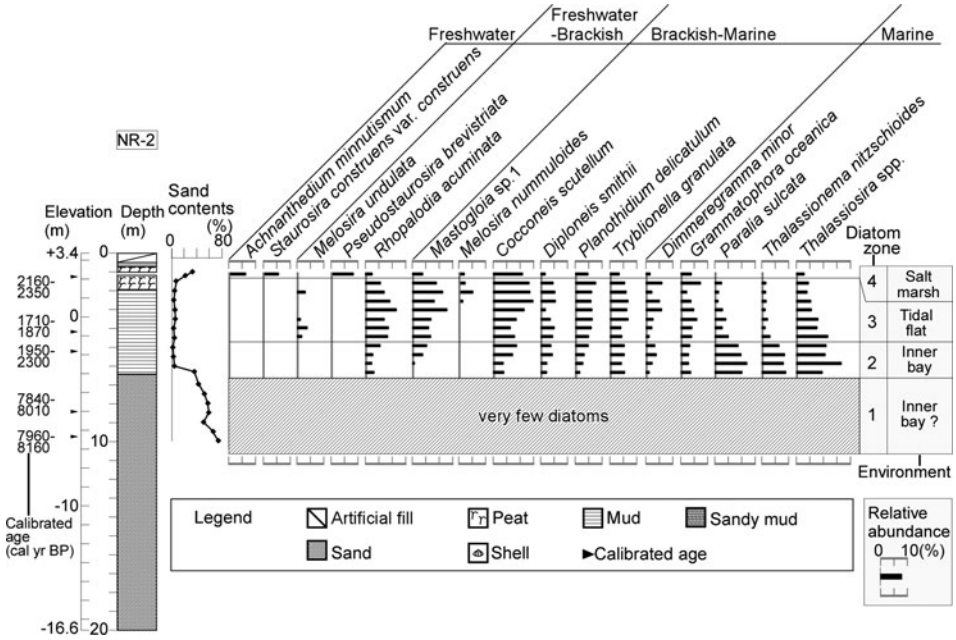

Figure 5. Stratigraphy, diatom assemblages, and ^{14}C ages in core NR-2.

2.5 m core depth (elevation −0.1 to −0.2 m); the environment changed to a freshwater marsh during the period 1260–1070 cal yr BP (2.2 m core depth; elevation 0.1 m).

Palaeoenvironments inferred from the lithology and diatom assemblages of NR-2

Core NR-2 (Fig. 5) consisted of muddy to sandy sediments. Relatively well-sorted fine to medium sand with shell fragments occurred from 20.0–6.7 m depth (sand content 44–75%) and an upward-fining sequence of fine sand from 6.7–6.3 m depth. The sediments consisted of mud from 6.3–1.9 m depth (sand content 2–37%), peat from 1.9–0.7 m depth, and organic-rich mud from 0.7–0.5 m depth. The boundary between the lower mud and the upper peat was gradual. Artificial fill deposits were recognised from 0.5–0 m depth.

We identified four diatom zones in core NR-2 (Fig. 5). The lowermost zone 1 consisted of medium or coarse sand and broken marine diatoms such as *Thalassiosira* spp. were slightly recognised; this zone was interpreted as a shallow marine, wave-influenced environment. Although diatom zone 1 contained nearly no diatoms, fragments of marine species such as *Cyclotella litoralis* and *Grammatophora* spp. were found, suggesting that it represents a marine environment. Diatom zone 2 was characterised by marine and brackish-marine diatoms such as *Thalassionema nitzschioides*, *Thalassiosira* spp., and *Cocconeis scutellum* and it consisted mainly of muddy sediments. Thus, it was interpreted as representing a shallow marine environment. In diatom zone 3, marine diatoms decreased and brackish-marine diatoms such as *Mastogloia* sp., *Planothidium delicatulum*, and *Tryblionella granulata* increased. Freshwater-brackish species such as *Rhopalodia acuminata* also increased; the lithology of this zone was organic mud and peaty deposits. Therefore, zone 3 represents muddy tidal flat and salt marsh environments. The uppermost zone 4 was characterised by freshwater, freshwater-brackish, and brackish-marine diatoms such as *Staurosira construens*, *Pseudostaurosira brevistriata*, and *Cocconeis scutellum*. The lithology of zone 4 was peat; thus, this zone represents a low-salinity salt marsh environment.

The lithologic and diatomaceous data suggest that the shoreline reached the NR-2 core site during the period 8200–8000 cal yr BP (10.0 m core depth; elevation -6.6 m). A subtidal environment prevailed at the core site from 8000 to 2000 cal yr BP, but by 1860 cal yr BP a tidal flat occupied the site; thus, during the period 1860–1710 cal yr BP (4.2 m depth; elevation -0.8 m) the core site was near mean sea level. Later, a salt marsh occupied the site (0.7–1.9 m core depth; elevation 2.7–1.5 m).

Palaeoenvironments inferred from the lithology and diatom assemblages of IB-1

Core IB-1 contained late Pleistocene and Holocene deposits (Fig. 6). The interval from 26.8–26.5 m consisted of peaty sediments (sand content 60%) overlying fine to medium sand from 27.0–26.8 m depth. The interval from 26.5–25.8 m depth consisted of sand (sand content 45–60%) overlying peat with an erosional contact. The sediments from 25.8–25.1 m depth consisted of peaty deposits (sand content 45%). The interval from 24.6–24.2 m depth consisted of muddy deposits and included a 0.1-m-thick unidentified late Pleistocene tephra layer (sand content 30%). The sediments beneath the mud consisted of sand or muddy sand

https://doi.org/10.1017/qua.2019.69 Published online by Cambridge University Press

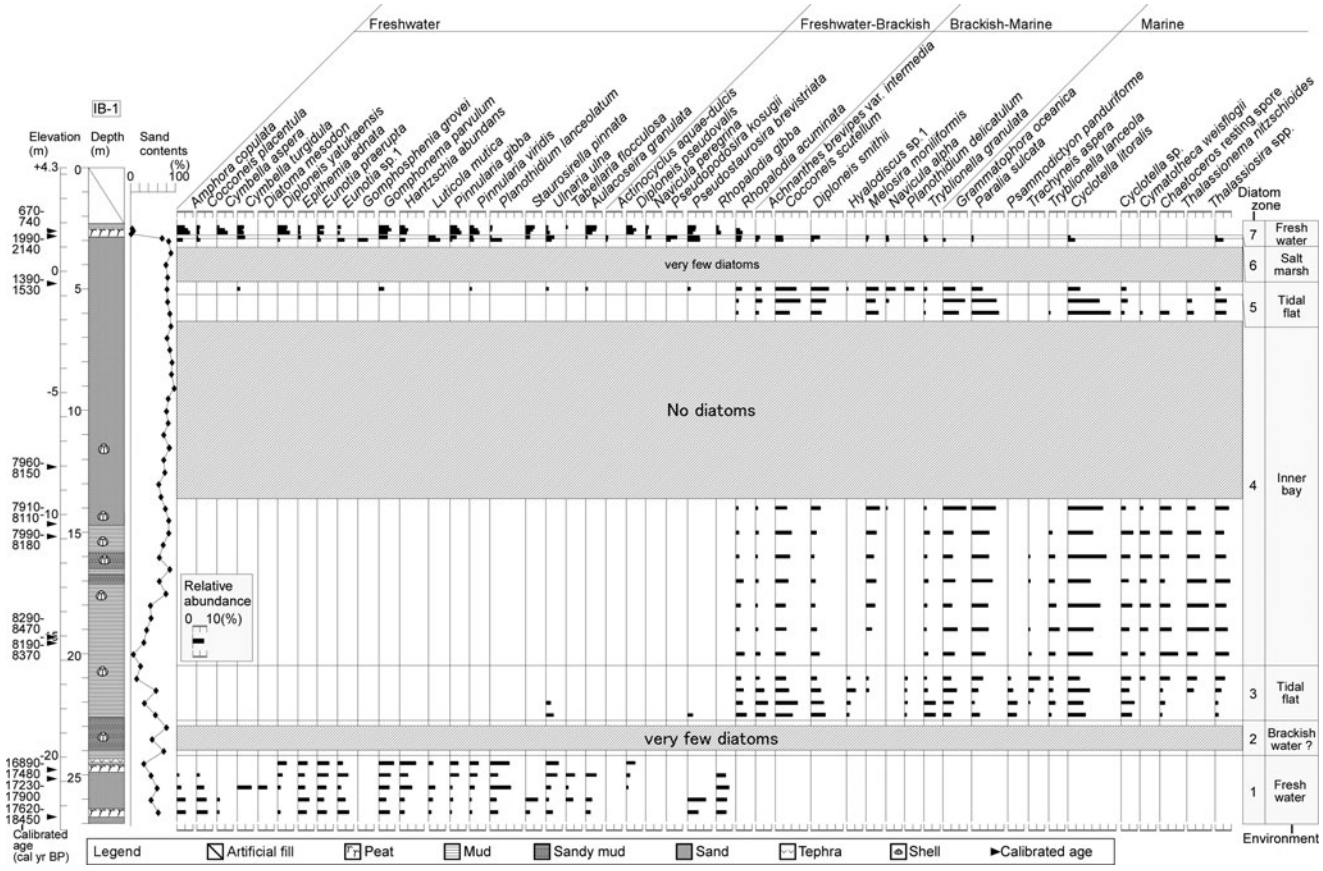

Figure 6. Stratigraphy, diatom assemblages, and ^{14}C ages in core IB-1.

with shell fragments (24.2–22.5 m depth; sand content 49–80%) overlying muddy deposits with an erosional contact. The interval from 22.5–18.6 m depth was mud with shell and shell fragments (sand content 14–57%). A sandy deposit (sand content 45%) was recognised in the upper muddy deposits and that from 18.2–16.7 m depth consisted of muddy sand with shells (sand content 44–78%). The interval from 16.7–16.0 m depth consisted of sand (sand content 88%). The interval from 16.0–15.0 m depth consisted of muddy sand with shells (sand content 64–73%). The interval from 15.0–2.9 m depth was sandy (sand content 74–93%) with some gravel from 7.0–6.2 m depth. The natural sediments consisted of mud from 2.5–2.4 m depth (sand content 4%) overlying peat from 2.9–2.5 m depth (sand content 1–70%). Artificial fill occupied the uppermost 2.4 m.

We identified diatom zones 1 to 7 in ascending order (Fig. 6). Zone 1 was characterised by freshwater diatoms such as *Planothidium lanceolatum* and *Gomphonema parvulum*; therefore, zone 1 represents a freshwater environment. Zone 2 above zone 1 was a sand deposit containing nearly no diatoms; however, a few broken frustules of brackish and marine diatoms were recognised; thus, this zone was probably an intertidal environment such as sand flat environment. Above the sand, zone 3 was characterised by intertidal diatoms such as *Diploneis smithii* and *Planothidium delicatulum* and was interpreted as a muddy tidal flat environment. Zone 4 was characterised by marine planktonic diatoms such as *Cyclotella litoralis*, *Thalassionema nitzschioides*, and *Thalassiosira* spp. and it lithologically mainly consisted of mud. Thus, zone 4 was interpreted as representing a marine environment such as an inner bay environment. In diatom zone 5, marine planktonic diatoms decreased and intertidal diatoms such as *Navicula alpha* and *Planothidium delicatulum* dominated the assemblage. Lithologically, it consisted mainly of sand. Therefore, this zone was interpreted as a sandy tidal flat environment. Zone 6 was characterised by freshwater and freshwater-brackish species, in particular, *Pseudopodosira kosugii*, and peat. Thus, this zone was a salt marsh very near the marine limit. Zone 7 was characterised by freshwater diatoms such as *Cymbella aspera* and *Diploneis yatukaensis* and a sandy lithology. Thus, it represents a freshwater environment.

The lithology and diatoms suggest that a freshwater environment prevailed from 18,000–17,000 cal yr BP. Thereafter, sea level rose and the environment changed to a subtidal, inner bay environment; at 8370 cal yr BP sea level was at 22.0 m core depth (elevation −17.7 m). Subsequently, a sandy tidal flat occupied the site, but its duration remains unknown because of a lack of dated samples. The subtidal environment changed to a sandy tidal flat environment by at least 1530 cal yr BP (4.8 m core depth; elevation -0.5 m). Salt marsh, indicating the marine limit, was found at 2.9 m core depth (elevation 1.4 m). The environment was a freshwater marsh during the period 1390–740 cal yr BP.

https://doi.org/10.1017/qua.2019.69 Published online by Cambridge University Press

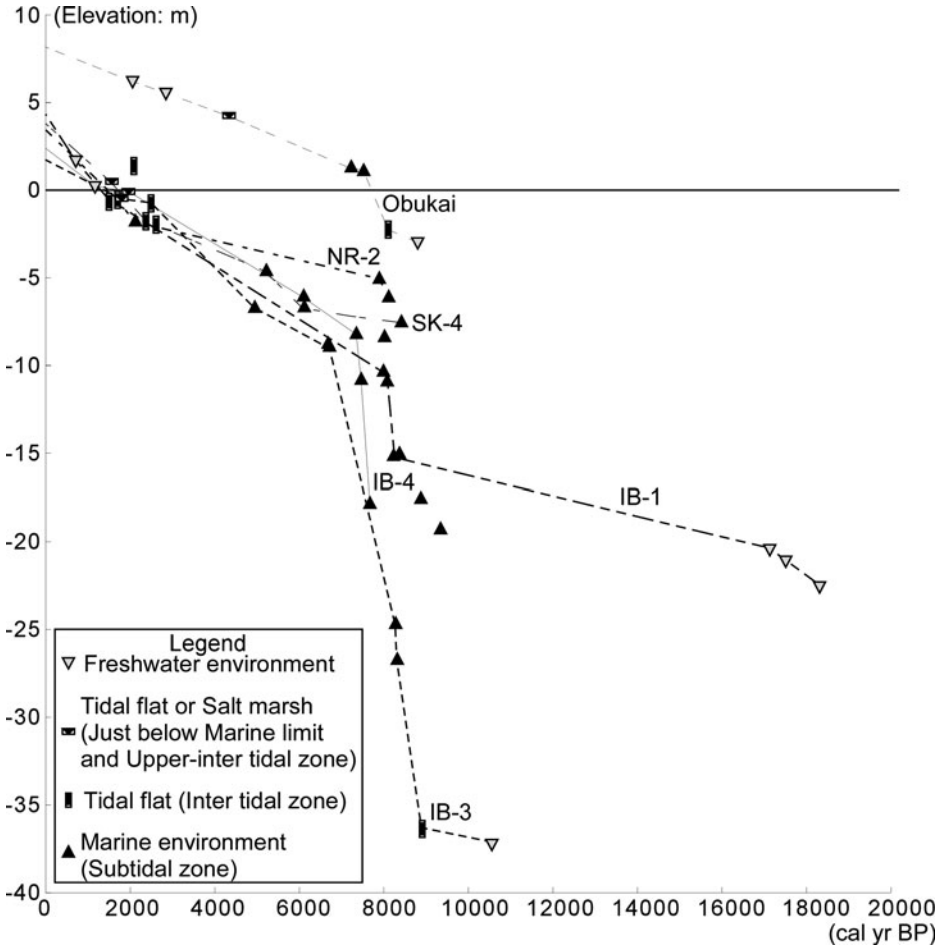

Figure 7. Sedimentation curve in IB-1, 3, and 4; NR-2; SK-4 (Chiba et al., 2016); and Obukai (index points based on Chiba [2014]).

DISCUSSION

Reconstruction of palaeogeographic changes in the northern Lake Inba area

We reconstructed the palaeogeography in the Lake Inba area using the diatomaceous and dating results of cores IB-1, -3, and -4 and NR-2. The lake outlet area was occupied by a freshwater environment from 18,000 to 9000 cal yr BP. In 9000 cal yr BP, seawater inundated the Lake Inba outlet area (IB-3 and -4), and until 8300 cal yr BP, the area from the outlet to the mouth of the Kashima River (IB-1) was an inner bay. Seawater influences in the present lake area continued until 1000 cal yr BP.

Sedimentation rates at the sites of cores IB-1, -3, -4 and NR-2 (Fig. 7) showed similar patterns. Before 10,000 cal yr BP, the sedimentation rate was 0.5–0.6 mm/yr. After seawater inundated the Lake Inba area, mainly owing to the Holocene transgression (9000–8000 cal yr BP), the sedimentation rate abruptly increased to 16.1–28.9 mm/yr at the core sites. It is a possible that a hiatus occurred around 8000 cal yr BP in NR-2 for the exceptionally low deposition rate tha was recognised. Then, from 8000–2000 cal yr BP, the sedimentation rates decreased to 0.6–2.4 mm/yr at the core sites. During the period 3000–2000 cal yr BP the sedimentation rate increased at only two of the core sites (from 1.2–3.1 mm/yr in IB-1 and from 0.6–1.2 mm/yr in NR-2). These sedimentation rate changes reflect the palaeogeographic changes that occurred in the study area.

The sediment supply for the Tone River over the past 13,000 years has been reconstructed by means of a simulation (Kubo et al., 2006). Although there was no major change in the amount of suspended sediment supplied during this period, the amount of bed load sediment was 97.7–115.3 kg/s from 8–6 ka and was lower (11.8–16.5 kg/s) from 4–0 ka. The amount of bed load sediment varied with changes in the riverbed slope and reached a maximum during the Holocene high stand (Kubo et al., 2006; Tanabe, 2019). The results of this study are not inconsistent with those of these previous studies.

Reconstruction of palaeoshoreline changes in the Lake Inba area

Next, we reconstructed the palaeoshoreline in the Lake Inba area using the results from cores IB-1, -3, and -4 and NR-2

https://doi.org/10.1017/qua.2019.69 Published online by Cambridge University Press

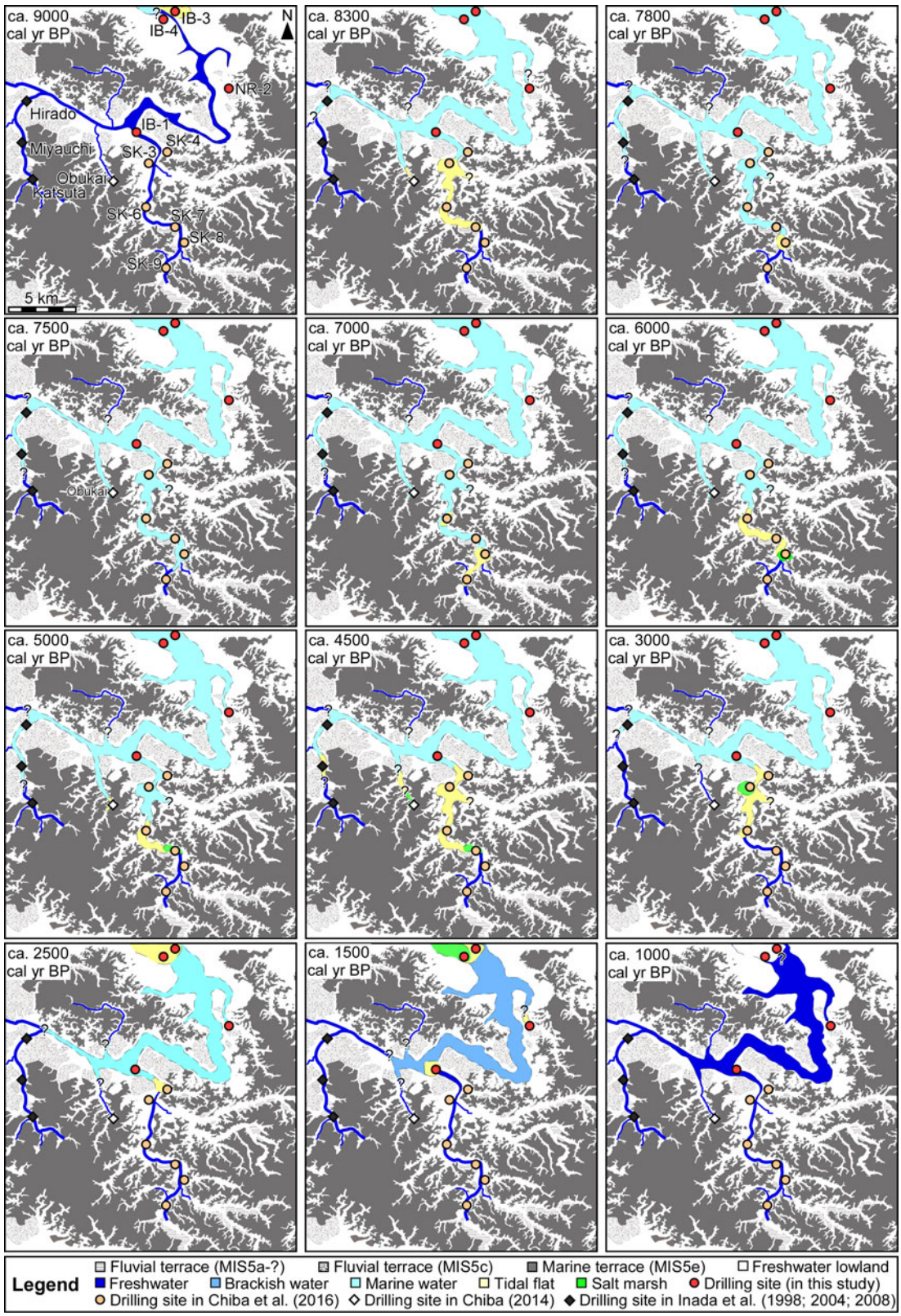

Figure 8. (color online) Palaeogeographic maps of Lake Inba area at at approximately 9000, 8300, 7800, 7500, 7000, 6000, 5000, 4500, 3000, 2500, 1500, and 1000 cal yr BP.

together with results reported by Chiba et al. (2011, 2016) and Inada et al. (1998, 2004, 2008; Fig. 8). The Lake Inba outlet area was characterised by a freshwater marsh until approximately 9000 cal yr BP. During the Holocene transgression, the palaeoshoreline, as indicated by the presence of a tidal flat environment, reached the IB-3 and -4 sites

https://doi.org/10.1017/qua.2019.69 Published online by Cambridge University Press

at approximately 9000 cal yr BP, but it did not reach the IB-1, SK-3, -4, and -6–8 sites until 8300 cal yr BP. The palaeoshoreline reached the NR-2 and Obukai sites at approximately 8000 cal yr BP (Chiba, 2014); at this time, the area between the lake outlet and the SK-7 site was characterised by a subtidal inner bay environment, which also extended to the Miyauchi site (Inada et al., 2008). By approximately 7000 cal yr BP, the palaeoshoreline had reached the SK-9 site and Obukai was in the inner bay (Chiba, 2014). Regression began after 6000 cal yr BP, and the salinity began to decrease at many sites, such as at SK-9 along the upper Kashima River. The tidal flat environment that had prevailed at SK-8 changed to a salt marsh, and at SK-7 and Obukai, the inner bay changed to a tidal flat (Chiba et al., 2016). As sea level continued to fall during the period 5000–4500 cal yr BP, the Kashima River area was characterised by less-saline environments: a freshwater marsh prevailed at SK-8, a salt marsh at Obukai (Chiba, 2014), and tidal flats at SK-3 and -4 (Chiba et al., 2016). During this period, brackish-marine diatoms such as *Diploneis smithii* and *Tryblionella granulata* increased at the Miyauchi site (Inada et al., 2008), suggesting that a tidal flat had formed. By 3000 cal yr BP, a freshwater environment prevailed at SK-7, Obukai, and Miyauchi and there was a salt marsh at SK-3. By 2600 cal yr BP, as sea level continued to fall, tidal flats were found at the IB-3 and -4, and NR-2 sites and a salt marsh had formed at the SK-4 site. In addition, the Daikatahanawa shell mound (Fig. 1c and d), which was composed mainly of *Corbicula japonica* shells, accumulated on the shore of Lake Inba near the NR-2 site during the Yayoi period (from several centuries BC to the third century AD; Chiba et al., 2011). *Corbicula japonica* is a bivalve that inhabits a brackish water environment; it has difficulty surviving in a marine environment (Tanaka, 1984). If *Corbicula japonica* occurred in Lake Inba during the Yayoi period, then the salinity of the lake at that time was lower than that typical of a marine environment. After approximately 1000 cal yr BP, a freshwater environment characterised the IB-1 and -4 sites. The timing of these changes is consistent with some historical documents (Yamaji, 2004). The changes in the species composition of Jomon shell mounds in the Lake Inba area are also consistent with these palaeoshoreline changes (Yoshino, 1998). These lines of evidence suggest that Lake Inba's change from a saline lagoon to a freshwater lake may have partly resulted from late Holocene sea-level changes and was not caused by the effects of the so-called Tonegawa Tosen, the artificial rerouting of the Tone River channel after AD 1594 (Inazaki et al., 2014). These results are consistent with the study of Lake Kasumigaura (Saito et al., 1990, 2016) and Kitaura (Fig. 1; Naya et al., 2007); desalination had progressed long before the two downstream side lakes. The Jinsokuzu map created in AD 1886 (Fig. 1c and d) shows a reverse delta in the lake outlet. This suggests that the sediment supply of the Tone River changed as a result of its artificial rerouting (Kusuda and Nirei, 1994).

Comparison of the timings of salinity changes in Lake Inba, Lake Kasumigaura, Lake Kitaura, and the Tone River lowland

In the inland lake, the timing of the salinity change is slightly later than Lake Kasumigaura and Kitaura during the Holocene transgression period (Fig. 9). The period was approximately 10,000–9000 cal yr BP and after which the inner bay environment expanded. In Lake Kasumigaura, the sea area expanded until approximately 4000 cal yr BP (Saito et al., 2016), but in Lake Inba it began to contract at approximately 5000 cal yr BP; the sea area also contracted from approximately 2500 to 2000 cal yr BP. At that time, a closed inner bay environment formed in Lake Kasumigaura. The desalination in Lake Inba was complete approximately 1000 yr; however, the influence of seawater remained in the downstream area and Lake Kasumigaura and Lake Kitaura (Naya et al., 2007; Naya, 2016; Saito et al., 2016). These differences reflect the respective positional relationships and the extended range of the tide level.

In the lowland along the Tone River, in the eastern part of the Lake Inba area, palaeogeographical changes associated with sea-level changes at approximately 7 ka were reconstructed by Tanabe et al. (2014). According to Tanabe et al. (2014), a spit or barrier formed in the river mouth area (the bay mouth area of the Palaeo-Kinu Bay; Fig. 1; Kikuchi, 1969; Saito et al., 1990). The tidal current reached more inland at 5 ka. Thereafter, the range that the tidal current reached moved to the seaward side because of the sea-level fall at 3 ka. The range also moved to the seaward side at 0.5 ka. The palaeogeography of the northern part of Lake Inba is also harmonious with the palaeogeographical changes reconstructed by Tanabe et al. (2014).

Residual subsidence rate in the northern Lake Inba area

Lakes Kasumigaura and Kitaura did not form via damming of sandbars in the lake inlets and outlets because of sea-level changes but as a result of tectonic subsidence, similar to Lake Bradley (Kelsey et al., 2005) in Oregon and Lakes Biwa (e.g., Tsutsui et al., 1990) and Mikata (e.g., Yasuda, 1982) in Japan. If Lake Inba, in a more inland area, formed via similar processes to these lakes, it is important to study the palaeoenvironmental reconstruction to identify the signal of subsidence and estimate the influence of the subsidence rate. Tectonic subsidence has been identified by the recognition of an abrupt increase in the sedimentation rate (Tanabe et al., 2009) or by lowering the levels of reconstructing points or a curves comparison between the level of sea-level index points or the reconstructing curve and the calculated or simulated sea-level curve or fitted global sea-level curve (Tanigawa et al., 2013; Okuno et al., 2014). The palaeosea-level change during the past 8500 yr in the northern part of Lake Inba area was reconstructed by Chiba et al. (2016). According to their work, the sea level reached −9.0 m

https://doi.org/10.1017/qua.2019.69 Published online by Cambridge University Press

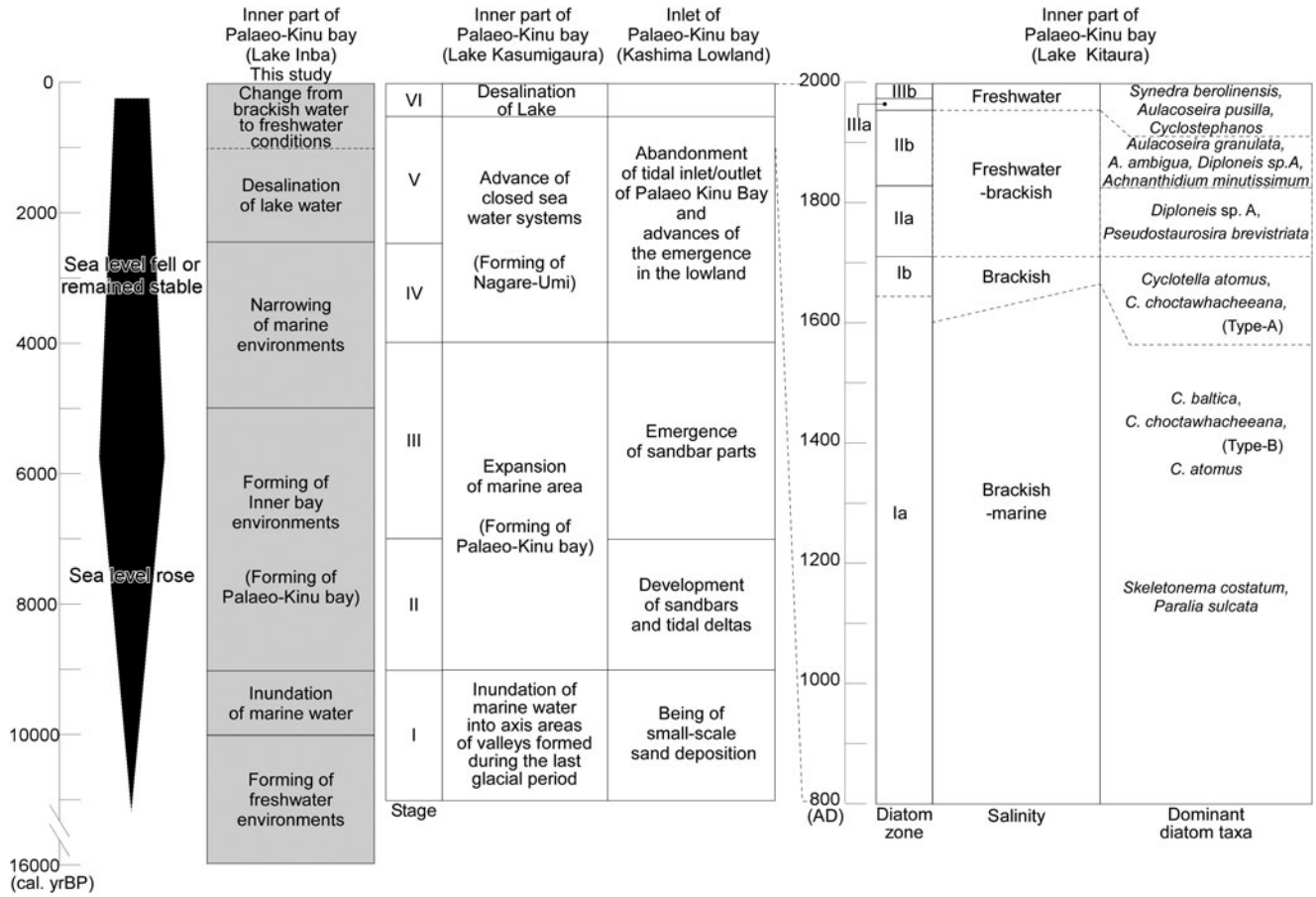

Figure 9. Comparison of the timing of salinity changes in Lake Inba, Lake Kasumigaura (Saito et al., 2016), and Lake Kitaura (Naya et al., 2007; Naya 2016; Ito et al., 2017).

elevation in 8550–8410 cal yr BP, and then reached the Holocene high stand of + 2.8 m in 6500–6400 cal yr BP. After that, the sea level started to decrease toward the present. However, the palaeo-sea-level before 8500 cal yr BP was not revealed. We added new sea-level index points into the sea-level curve (Chiba et al., 2016), and revised it (Fig. 10). The possibility that an increase in the sedimentation rate and a sea-level rise in this study area is a result of subsidence centres around the IB-3 site.

Okuno et al. (2014) examined the tectonic crustal movements along the Japanese coastlines on three timescales (~50, ~6000, and ~125,000 yr) using several sets of sea-level observations and model predictions based on glacio-hydro isostatic adjustment processes and recent melting of mountain glaciers and the Antarctic and Greenland ice sheets. The sea-level observations applied to infer the rates of crustal movement for ~50, ~6000, and ~125,000 yr are tide gauge records at 34 sites, Holocene RSL changes at 43 sites, and the altitudes of marine terraces formed during the Last Interglacial phase (Koike and Machida, 2001), respectively. Okuno et al. (2014) calculated a relative sea-level curve based on geophysical modelling including glacio-hydro isostatic adjustment along the Japan coast. The mean sea level in Tokyo at 9 ka was concluded to have been −10.7 m by Okuno et al. (2014); however, in this study, the sea level is inferred to have been -36.3 m during this period. Tanabe et al. (2015) added new sea-level index points to the sea-level curve of Endo et al. (1989) for the Tokyo and Nakagawa lowlands and obtained additional details of the changes during the sea-level rise, confirming the work of Ishihara et al. (2012). Tanabe (2019) further developed this research (Tanabe et al., 2015; Tanabe and Nakashima, 2016) and drew a new sea-level curve. Based on the index points of Tanabe et al. (2015) and Tanabe (2019), the mean sea level at 9 ka was -16.0 m.

The mean subsidence rate was calculated from the amount of subsidence divided by the time over which that subsidence occurred; this information was obtained from the elevations and ages of each sample. We adopted $E_1 = -10.7$ m (Okuno et al., 2014), $E_2 = -36.3$ m, and $T = 9000$ yr, which yielded:

$$\frac{(-10.7 - (-36.3))}{9000} \fallingdotseq 2.8 \text{ mm/yr}$$

As the index point set by Chiba et al. (2016) includes an error of at least ± 3.3 m, the actual value may have been less than 2.8 mm/yr. However, even if this error is considered, it is certain that subsidence had occurred. Similar calculations revealed that the northern part of the Lake Inba area subsided at a rate of 2.3 mm/yr relative to the Tokyo and Nakagawa

https://doi.org/10.1017/qua.2019.69 Published online by Cambridge University Press

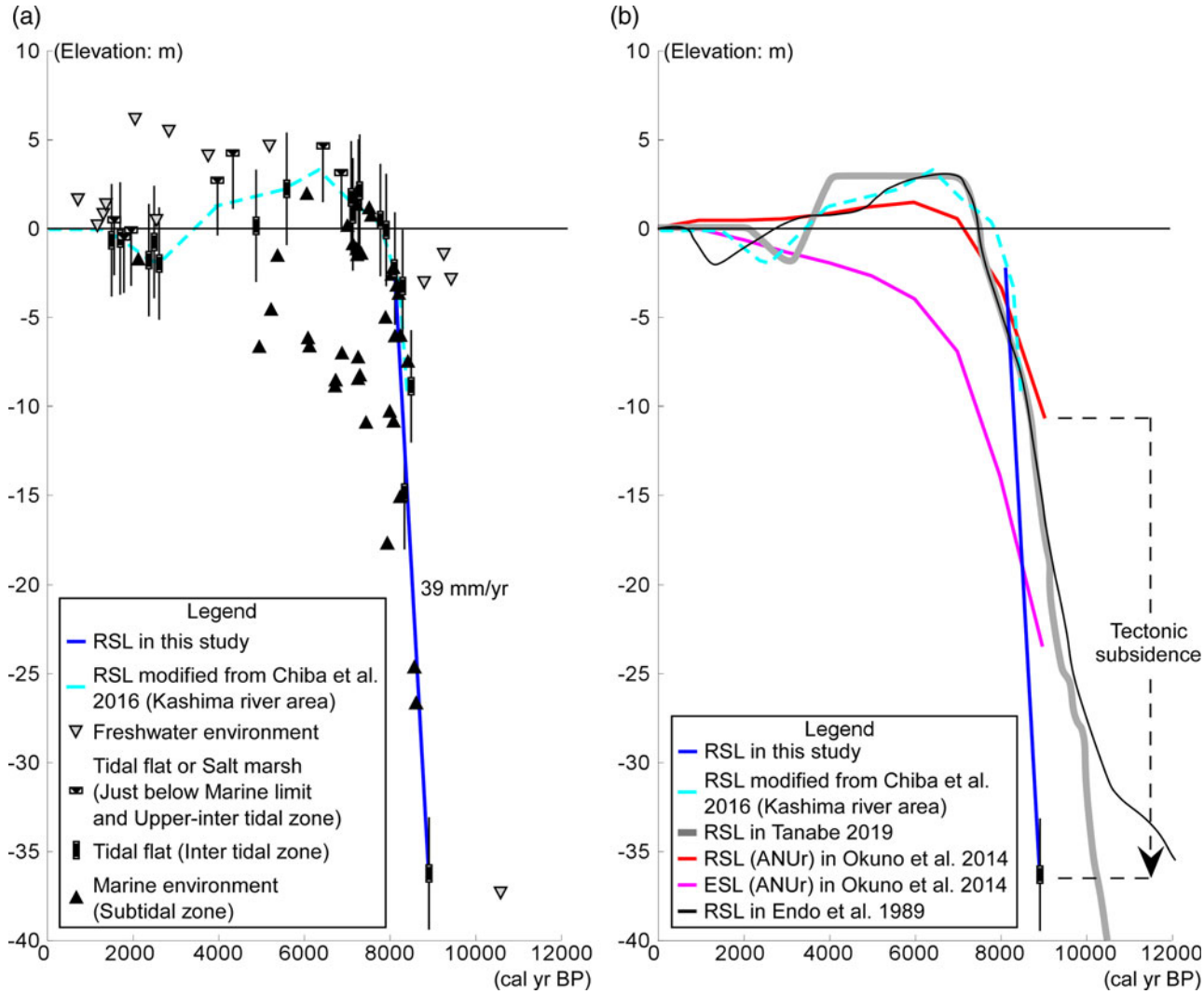

Figure 10. (color online) (a) Relationship of relative sea-level changes among the southern part of Lake Inba area and Obukai and Kashima River areas (southern part of Lake Inba area; Chiba et al., 2016). (b) Relationship of relative sea-level changes among this study data, corrected values (modified from Chiba et al. [2016]), the modelled sea-level curve (Okuno et al., 2014), and the sea-level curve in the Tokyo lowland (Endo et al., 1989; Tanabe, 2019).

lowlands. In addition, the timing of sea-level rise slightly differs from that in the Kashima River area (Chiba et al., 2016), which was 8500–7000 cal yr BP. This difference may reflect the difference in crustal movement patterns between the northern downstream (subsiding) and the southern upstream (uplifted) parts of the Lake Inba area (Fig. 1).

The minute influence of the subsidence was also recognised at the IB-4 site and decreased toward the south part of the Lake Inba area reviewing the cross section and isochrones (Fig. 2 and 10). On the other hand, the reduction of the scale of the water body was a result of the regression after Holocene transgression. This reconstructed palaeo environmental change is consistent with what is written in historical literature (Oya, 1969; Yamaji, 2004). If the poor drainage in this area and associated long-term bay formation during the late Holocene was the effect of subsidence as shown in this study, this does not contradict these historical records; however, the timing of the subsidence event is unknown. Namely, one possible reason that Palaeo-Kinu Bay (or Sea of Katori) was a long narrow lake until the Medieval period is subsidence. Additionally, formation of the reverse delta shown in the Jinsokuzu map developed in AD 1886 (Fig. 1c and d) possibly reflected the sediment supply resulting from subsidence. Because the influence of sediment compaction was not considered, it is possible that the estimated subsidence rate is a slight overestimation. However, subsidence in the northern part of the Lake Inba area is not inconsistent with the Quaternary tectonics and active geological structures estimated by Kaizuka (1987).

CONCLUSION

To reconstruct the palaeogeographic and lake environmental changes resulting from the Holocene transgression and

https://doi.org/10.1017/qua.2019.69 Published online by Cambridge University Press

residual subsidence in the eastern Kanto Plain of central Japan, we analysed four drill cores obtained from northern part of the Lake Inba area and reviewed other core data from the southern part of the area. The palaeogeographic history resulting from sea-level changes since the Late Pleistocene was reconstructed. We determined that seawater inundation into the Lake Inba area during the Holocene transgression occurred approximately 9000 yr and the environment in Lake Inba changed from brackish to freshwater no later than 1000 yr. We also recognised the occurrence of residual subsidence during the Holocene (at a rate of 2.8 mm/yr) by comparing the model data with our palaeosea-level change data. Thus, comparison of palaeosea-level reconstructions based on modelling and the diatom fossil record is effective in interpreting long-term subsidence during the Holocene.

ACKNOWLEDGMENTS

We thank Mr. Tokuo Fujimori to accommodate in core sampling. We also thank Dr. Jun'ichi Okuno for referring to the model data in Kanto. We also thank Dr. Toshihiko Sugai, Dr. Susumu Tanabe, Dr. Arata Momohara, Dr. Shigehiro Fujino, Dr. Takahiro Shiina, and Dr. Naomitsu Yamaji for valuable discussions to improve this study. We are very grateful to Dr. Kazuo Masubuchi, Dr. Taiji Kurozumi, Dr. Kunio Yoshida, Mr. Takeji Toizumi, Mr. Kensuke Tsurumaki, and Mr. Tatsuaki Hara for helping with the sampling. And we also thank Dr. Takato Takemura, Dr. Yuriko Nakao, Dr. Akira Ono, and Mr. Taro Kannari for help and use of measuring instruments. We would like to acknowledge Dr. Taisuke Ohtsuka, Dr. Itsuki Suto, and Dr. Tsuyoshi Watanabe for discussions about diatoms. This work was supported, in part, by the Academic Frontier Project for private universities and the Program to Disseminate Tenure Tracking System, MEXT, Japan.

SUPPLEMENTARY MATERIAL

The supplementary material for this article can be found at https://doi.org/10.1017/qua.2019.69

REFERENCES

Chiba, T., 2014. Taphonomy of diatoms and problems of paleoenvironmental reconstruction in coastal areas using diatom assemblages. [In Japanese with English abstract.] *Diatom* 30, 86–103.

Chiba, T., Kanauchi, A., Kamiya, C., Sugihara, S., 2011. Locational environment of Daikatahanawa shell mound and paleo environmental changes in Paleo Inba bay. *The Environmental Development and Human Activity* 5, 67–83.

Chiba, T., Nishimura, Y., Ohtsuka, T., 2018. Fossil diatom assemblages during the last millennium in the Toberi River mouth area, Hokkaido, Japan. *Diatom* 34, 8–29.

Chiba, T., Sawai, Y., 2014. Reexamination and updating of diatom species for paleoenvironmental reconstructions. [In Japanese with English abstract.] *Diatom* 30, 17–30.

Chiba, T., Sugihara, S., Matsushima, Y., Arai, Y., Endo, K., 2016. Reconstruction of Holocene relative sea-level change and residual uplift in the Lake Inba area, Japan. *Palaeogeography, Palaeoclimatology, Palaeoecology* 441, 982–996.

Chiba Prefectural Environmental Research Center, 2016. Wide-area river improvement and integrated river environmental improvement project: Class A river, Lake Inba (accessed April 2019). https://www.pref.chiba.lg.jp/wit/.

Clark, J.A., Farrell, W.E., Peltier, W.R., 1978. Global changes in postglacial sea level: A numerical calculation. *Quaternary Research* 9, 265–287.

Cocquyt, C., Olodo, I., Abou, Y., 2018. Transfer of *Navicula elegantoides* Hustedt to the genus *Pinnunavis* (*Naviculaceae*, Bacillariophyta). *Notulae Algarum* 66, 1–4.

Editorial Committee of the History of Noda-shi, 2010. *Paleoenvironmental Studies and Borehole Logs in Noda-shi*. [In Japanese.] Vol.1, Editorial Committee of the History of Noda-shi, Chiba.

Endo, K., Kosugi, M., Matsushita, M., Miyaji, N., Hishida, R., Takano, T., 1989. Holocene environmental history in and around the Paleo-Nagareyama Bay, central Kanto Plain. [In Japanese with English abstract.] *The Quaternary Research* (*Daiyonki-Kenkyu*) 28, 61–77.

Endo, K., Sekimoto, K., Takano, T., 1982. Holocene stratigraphy and paleoenvironments in the Kanto Plain, in relation to the Jomon Transgression. *Proceedings of the Institute of Natural Sciences, Nihon University* 21, 37–54.

Endo, K., Sekimoto, K., Takano, T., Suzuki, M., Hirai, Y., 1983. Holocene and latest Pleistocene deposits in the Kanto Plain, Central Japan. [In Japanese with English abstract.] *Uaban Kubota* 21, 26–43.

García-Artola, A., Stéphan, P., Cearreta, A., Kopp, R.E., Khan, N.S., Horton, B.P., 2018. Holocene sea-level database from the Atlantic coast of Europe. *Quaternary Science Reviews* 196, 177–192.

Hashima, A., Sato, T., Sato, H., Asao, K., Furuya, H., Yamamoto, S., Kameo, K., *et al*., 2016. Simulation of tectonic evolution of the Kanto Basin of Japan since 1 Ma due to subduction of the Pacific and Philippine Sea plates and the collision of the Izu-Bonin arc. *Tectonophysics* 679, 1–14.

Hasle, G.R., 1978. Some freshwater and brackish water species of the diatom genus *Thalassiosira* Cleve. *Phycologia* 17, 263–292.

Horton, B.P., Shennan, I., Bradley, S.L., Cahill, N., Kirwan, M., Kopp, R.E., Shaw, T.A., 2018. Predicting marsh vulnerability to sea-level rise using Holocene relative sea-level data. *Nature Communications* 9, 2687. http://dx.doi.org/10.1038/s41467-018-05080-0.

Idei, M., Osada, K., Sato, S., Toyoda, K., Nagumo, T., Mann, D.G., 2012. Gametogenesis and Auxospore Development in *Actinocyclus* (Bacillariophyta). *PloS One* 7, e41890. http://dx.doi.org/10.1371/journal.pone.0041890.

Inada, A., Ohama, K., Shimamura, K., 1998. Vegetational history since the latter period of the last glacial age around the lowland along the Shinkawa river in Yachiyo City, Chiba Prefecture, Central Japan. [In Japanese with English abstract.] *The Quaternary Research* (*Daiyonki-Kenkyu*) 37, 283–298.

Inada, A., Saito, T., Nirei, T., Nishimura, S., Ohama, K., Kaneko, S., Kaneko, Y., Shimamura, K., Shimizu, S., 2008. Holocene vegetational history and rice cultivation in the Shinkawa lowland, Yachiyo City, Chiba Prefecture, central Japan. [In Japanese with English abstract.] *The Quaternary Research* (*Daiyonki-Kenkyu*) 47, 313–327.

Inada, A., Saito, T., Ohama, K., Kaneko, S., Shimamura, K., Shimizu, S., Natsuaki, M., 2004. Paleoenvironmental transitions in the Shinkawa Lowland in Yachiyo City, Chiba Prefecture, Central Japan, since ca. 4,500 yr BP. [In Japanese with English abstract.] The Quaternary Research *(Daiyonki-Kenkyu)* 43, 1–14.

Inazaki, T., Ota, Y., Maruyama, S., 2014. The largest and longest project in Japan–spanning over 400 years river improvement works in the Kanto Plain and constraints of tectonic setting. [In Japanese with English abstract.] *Journal of Geography* (*Chigaku Zasshi*) 123, 401–433.

Ishihara, T., Toshihiko Sugai, T., Hachinohe, S., 2012. Fluvial response to sea-level changes since the latest Pleistocene in the near-coastal lowland, central Kanto Plain, Japan. *Geomorphology* 147–148, 49–60.

Itoh, N., Naya, T., Kanai, Y., Kumon, F, Amano, K., 2017. Historical changes in the aquatic environment and input of polycyclic aromatic hydrocarbons over 1000 years in Lake Kitaura, Japan. *Limnology* 18, 51–62.

Iwasaki, N., Sprague, S.D., Koyanagi, T., Furuhashi, T., Yamamoto, S., 2009. Development of the historical agro-environment browsing system constructed by FOSS4G. *Theory and Applications of GIS* 17, 83–92

Kaizuka, S., 1987. Quaternary crustal movements in Kanto, Japan. [In Japanese with English abstract.] *Journal of Geography* (*Chigaku Zasshi*) 96, 223–240.

Kaizuka, S., Koike, K., Endo, K., Yamazaki, H., Suzuki, T. (Eds.), 2000. *Regional Geomorphology of the Japanese Islands, Vol.4, Geomorphology of Kanto and Izu-Ogasawara*. University of Tokyo Press, Tokyo.

Kashima, K., Nemoto, K., Kobayashi, S., 1988. The Holocene successive change of diatom assemblages of drilling core samples in Lake Tega, Kanto Plain, Japan. *Diatom* 4, 61–65.

Kelsey, H.M., Nelson, A.R., Hemphill-Haley, E., Witter, R.C., 2005. Tsunami history of an Oregon coastal lake reveals a 4600 yr record of great earthquakes on the Cascadia subduction zone. *GSA Bulletin* 117, 1009–1032.

Khan, N.S., Ashe, E., Shaw, T.A., Vacchi, M., Walker, J., Peltier, W.R., Kopp, R.E., Horton, B.P., 2015. Holocene relative sea-level changes from near-, intermediate-, and far-field locations. *Current Climate Change Reports* 1, 247–262.

Kikuchi, T., 1969. Geomorphic development of the Kashima Lowland, Ibaraki Prefecture. *Geographical Reports of Tokyo Metropolitan University* 4, 23–32.

Koike, K., Machida, H., 2001. *Atlas of Quaternary Marine Terraces in the Japanese Islands*. University of Tokyo Press, Tokyo.

Komatsubara, J., Ishihara, Y., Ishihara, T., Kazaoka, O., Mizuno, K., 2017. Relationship between liquefaction damage and structure of lithological heterogeneity of Holocene postglacial deposits in the downstream basin of the Tone River, central Japan. [In Japanese with English abstract.] *Journal of Geography* (*Chigaku Zasshi*) 126, 715–730

Krammer, K., 2000. *Diatoms of Europe. Diatoms of the European Inland Waters and Comparable Habitats. Vol. 1. The genus* Pinnularia. ARG Gantner-Verlag KG, Ruggell, Liechtenstein.

Krammer, K., Lange-Bertalot, H., 1986. Bacillariophyceae. 1. Naviculaceae. In: *Süsswasserflora von Mitteleuropa*. Ettl, H., Gerloff, J., Heyning, H., Mollenhauer, D. (Eds.), Gustav Fischer Verlag, Jena.

Krammer, K., Lange-Bertalot, H., 1988. Bacillariophyceae 2. Teil: Bacillariaceae, Epithemiaceae, Sururellaceae. In: *Süßwasserflora von Mitteleuropa*. Ettl, H., Gerloff, J., Heyning, H., Mollenhauer, D. (Eds.), Gustav Fischer Verlag, Jena.

Krammer, K., Lange-Bertalot, H., 1991a. Bacillariophyceae 3. Teil: Centrales, Fragilariaceae, Eunotiaceae. In: *Süßwasserflora von Mitteleuropa*. Ettl, H., Gerloff, J., Heyning, H., Mollenhauer, D. (Eds.), Gustav Fischer Verlag, Jena.

Krammer, K., Lange-Bertalot, H., 1991b. Bacillariophyceae 4. Teil: Achnanthaceae, Kritische Ergänzungen zu Navicula (Lineolatae) und Gomphonema. In: *Süßwasserflora von Mitteleuropa*. Ettl, H., Gerloff, J., Heyning, H., Mollenhauer, D. (Eds.), Gustav Fischer Verlag, Jena.

Kubo, Y., Syvitski, J.P.M., Tanabe, S., 2006. An application of the hydrologic model HYDROTREND to the paleo-Tonegawa: numerical estimates of sediment discharge for the last 13,000 years. [In Japanese with English abstract.] *The Journal of the Geological Society of Japan* 112, 719–729.

Kusuda, T., Nirei, H., 1994. Geological history and characteristics of Imbanuma Reservoir. [In Japanese.] *Inbanuma-Shizen to Bunka-* No.1, 1–6.

Lambeck, K., Rouby, H., Purcell, A., Sun, Y., Sambridge, M., 2014. Sea level and global ice volumes from the Last Glacial Maximum to the Holocene. *Proceedings of the National Academy of Sciences of the United States of America* 111, 15296–15303.

Lisiecki, L.E., Raymo, M.E., 2005. A Pliocene-Pleistocene stack of 57 globally distributed benthic D18O records. *Paleoceanography* 20. http://dx.doi.org/10.1029/2004PA001071.

Masubuchi, K., Sugihara, S., 2010. Holocene paleoenvironmental changes and the formation of the shell mounds in the lower area of Tama River. [In Japanese.] *The Environmental Development and Human Activity* 4, 67–83.

Matsuda, T., Ota, Y., Ando, M., Yonekura, N., 1978. Fault mechanism and recurrence time of major earthquakes in southern Kanto district, Japan, as deduced from coastal terrace data. *Geological Society of America Bulletin* 89, 1610–1618.

Nagumo, T., 2003. Taxonomic studies of the subgenus Amphora Cleve of the genus *Amphora* (Bacillariophyceae) in Japan. Bibliotheca Diatomologica Vol.49. J. Cramer, Berlin and Stuttgart.

Naish, T.R., Wilson, G.S., 2009. Constraints on the amplitude of Mid-Pliocene (3.6–2.4 Ma) eustatic sea-level fluctuations from the New Zealand shallow-marine sediment record. *Philosophical Transactions of the Royal Society A* 367, 169–187.

Nakada, M., Lambeck, K., 1989. Late Pleistocene and Holocene sea-level change in the Australian region and mantle rheology. *Geophysical Journal International* 96, 497–517.

Nakata, T., Koba, M., Imaizumi, T., Jo, W.R., Matsumoto, H., Takeshi Suganuma, T., 1980. Holocene marine terraces and seismic crustal movements in the southern part of Boso Peninsula, Kanto, Japan. [In Japanese with English abstract.] *Geographical Review of Japan* 53, 29–44.

National Institute for Agro-Environmental Sciences, 2016. Historical Agro-Environmental Browsing System and Dissemination of Rapid Survey Map (accessed April 2019). http://habs.dc.affrc.go.jp.

Naya, T., 2016. Paleoenvironmental changes reconstructed from lake bottom sediment records: paleolimnological studies on Lake Kasumigaura, Ibaraki Prefecture, Japan. [In Japanese.] *Journal of Japan Society on Water Environment* 39, 270–273.

Naya, T., Tanimura, Y., Kanai, Y., Kumon, F., Amano, K., 2007. Natural and anthropogenic aquatic environmental changes reconstructed by paleolimnological analyses in Lake Kitaura, central Japan. *Journal of Paleolimnology* 37, 547–563.

Noda, A., Miyauchi, T., Sato, T., Matsu'ura, M., 2018. Modelling and simulation of Holocene marine terrace development in Boso Peninsula, central Japan. *Tectonophysics* 731–732, 139–154.

Okuno, J., Nakada, M., Ishii, M., Miura, H., 2014. Vertical tectonic crustal movements along the Japanese coastlines inferred from late Quaternary and recent relative sea-level changes. *Quaternary Science Reviews* 91, 42–61.

https://doi.org/10.1017/qua.2019.69 Published online by Cambridge University Press

Ota, Y., Matsushima, Y., Miyoshi, M., Kashima, K., Maeda, Y., Moriwaki, H., 1985. Holocene environmental changes in the Choshi Peninsula and its surroundings, easternmost Kanto, central Japan. [In Japanese with English abstract.] *The Quaternary Research* (*Daiyonki-Kenkyu*) 24, 13–29.

Ota, Y., Umitsu, M., Matsushima, Y., 1990. Recent Japanese research on relative sea level changes in the Holocene and related problems review of studies between 1980 and 1988. [In Japanese with English abstract.] *The Quaternary Research* (*Daiyonki-Kenkyu*) 29, 31–48.

Oya, M., 1969. Geomorphology and flooding of the plain in the middle and lower reaches of the Tone River in Kanto Plain. [In Japanese with English abstract.] *Journal of Geography* (*Chigaku Zasshi*) 78, 341–354.

Reimer, P.J., Baillie, M.G.L., Bard, E., Bayliss, A., Beck, J.W., Bertrand, C.J.H., Blackwell, P.G., *et al*., 2004. IntCal04 terrestrial radiocarbon age calibration, 0–26 cal kyr BP. *Radiocarbon* 46, 1029–1058.

Saito, Y., 1995. High-resolution sequence stratigraphy of an incised-valley fill in a wave- and fluvial-dominated setting: latest Pleistocene-Holocene examples from the Kanto Plain, central Japan. *The Memoirs of the Geological Society of Japan* 45, 76–100.

Saito, Y., Ikehara, K., Tamura, T., 2016. Coastal geology and oceanography. In: Moreno, T., Wallis, S.R., Kojima, T., Gibbons, W. (Eds), *The Geology of Japan*. Geological Society of London, London, pp. 409–430.

Saito, Y., Inouchi, Y., Yokota, S., 1990. Coastal lagoon evolution influenced by Holocene sea-level changes, Lake Kasumigaura, Central Japan. [In Japanese with English abstract.] *The Memoirs of the Geological Society of Japan* 36, 103–118.

Sato, H., Okuno, J.Nakada, M., Maeda, Y., 2001. Holocene uplift derived from relative sea-level records along the coast of western Kobe, Japan. *Quaternary Science Reviews* 20, 1459–1474.

Sawai, Y., 2001. A review on tidal-wetland diatoms as a paleo-sea-level reconstruction at Japanese estuaries. *Japanese Journal of Phycology* 49, 185–191.

Sawai, Y., Nagumo, T., 2003. Diatom (Bacillariophyceae) flora of salt marshes along the Pacific coast of eastern Hokkaido, northern Japan. *Bulletin of the Nippon Dental University General Education* 32, 93–108

Shennan, I., 1982. Interpretation of Flandrian sea-level data from the Fenland, England. *Proceedings of the Geologists' Association* 93, 53–63.

Shishikura, M., 2003. Cycle of interplate earthquake along the Sagami Trough, deduced from tectonic geomorphology. [In Japanese with English abstract.] *Bulletin of the Earthquake Research Institute* 78, 245–254.

Shishikura, M., 2014. History of the paleo-earthquakes along the Sagami Trough, central Japan: review of coastal paleoseismological studies in the Kanto region. *Episodes* 37, 246–257.

Stuiver, M., Braziunas, T.F., 1993. Modeling atmospheric ^{14}C Influences and ^{14}C Ages of Marine Samples to 10,000 BC. *Radiocarbon* 35, 137–189.

Sugihara, S., 1970. Geomorphological developments of the western Shimosa upland in Chiba Prefecture, Japan. *Geographical Review of Japan* 43, 703–718 (in Japanese with English abstract).

Sugihara, S., Kurozumi, T., Horikoshi, M., 2011. Fundamental geological survey for paleoenvironmental reconstruction in Lake Inba area. *The Environmental Development and Human Activity* 5, 32–66.

Sugimura, A., Naruse, Y., 1954. Changes in sea level, seismic upheavals, and terraces in the southern Kanto region, Japan (I). *Journal of Geology and Geography* 24, 101–113.

Takada, T., Uwagawa, M., Asada, K., Sato, N., Kudara, T., 1971. Research, design and construction of the embankment of the Lake Inba area. [In Japanese.] *Journal of the Agricultural Engineering Society, Japan* 39, 5–20.

Tanabe, S., 2019. Formation mechanisms of the post-LGM incised-valley fills beneath the Tokyo and Nakagawa lowlands, central Japan. [In Japanese with English abstract.] *The Journal of the Geological Society of Japan* 125, 55–72.

Tanabe S., Miyata, Y. Nakashima R., Mizuno, K., 2014. Result of sediment core analysis of the post-LGM incised-valley fills in the left bank area of the Tone River. [In Japanese with English abstract.] *Reports of Research and Investigation on Multiple Geological Hazards Caused by Huge Earthquakes, GSJ Interim Report* 66, 297–318.

Tanabe, S., Nakanishi, T., Ishihara, Y., Nakashima, R., 2015. Millennial-scale stratigraphy of a tide-dominated incised valley during the last 14 kyr: spatial and quantitative reconstruction in the Tokyo Lowland, central Japan. *Sedimentology* 62, 1837–1872.

Tanabe, S., Nakashima, R., 2016. Lithofacies, biofacies and radiocarbon dates of the Alluvium in core sediments obtained from the Tamagawa Lowland, central Japan. [In Japanese with English abstract.] Annual Report of Investigations on Geology and Active Faults in the Coastal Zone of Japan *(*FY*2015),* GSJ Interim Report 71, 109–120.

Tanabe, S., Tateishi, M., Shibata, Y., 2009. The sea-level record of the last deglacial in the Shinano River incised-valley fill, Echigo Plain, central Japan. *Marine Geology* 266, 223–231.

Tanaka, Y., 1984. Salinity tolerance of the brackish-water Clam, Cobicula japonica Prime. *Bulletin of National Research Institute of Aquaculture* 6, 29–32.

Tani, K., 2015. Proceedings of the General Meeting of the Association of Japanese Geographers. The Association of Japanese Geographers, Tokyo.

Tani, K., 2016. Web Site to Draw Contour Lines of Japan (accessed April 2019). http://ktgis.net/lab/etc/webcontour/.

Tanigawa, K., Hyodo, M., Sato, H., 2013. Holocene relative sea-level change and rate of sea-level rise from coastal deposits in the Toyooka Basin, western Japan. *The Holocene* 23, 1039–1051.

Tanimura, Y., Sato, H., 1997. *Pseudopodosira kosugii*: a new Holocene diatom found to be a useful indicator to identify former sea-levels. *Diatom Research* 12, 357–368.

Tsutsui, T., 1990. Three-dimensional subsurface structure beneath the Hino river fiat, south-east shore of Lake Biwa, central Japan. *Journal of Physics of the Earth* 38, 403–429.

Vacchi, M., Engelhart, S.E., Nikitina, D., Ashe, E.L., Peltier, W.R., Roy, K., Kopp, R.E., Horton, B.P., 2018. Postglacial relative sea-level histories along the eastern Canadian coastline. *Quaternary Science Reviews* 201, 124–146.

Watanabe, T., Tanaka, J., Reid, G., Kumada, M., Nagumo, T., 2013. Fine structure of *Delphineis minutissima* and *D. surirella* (Rhaphoneidaceae). *Diatom Research* 28, 445–453.

Witkowski, A., Lange-Bertalot, H., Metzeltin, D., 2000. Diatom Flora of Marine Coasts 1. In Lange-Bertalot, H., (Ed.), *Iconographia Diatomologica Vol.7*. Koeltz Scientific Books, Königstein.

Yamaji, N., 2004. "Ikawano-shiri" and "Katorino-Umi". [In Japanese.] *Kodaikotsu-Kenkyu* 13, 3–20.

https://doi.org/10.1017/qua.2019.69 Published online by Cambridge University Press

Yasuda, Y., 1982. Pollen analytical study of the sediment from the Lake Mikata in Fukui Prefecture, Central Japan. [In Japanese with English abstract.] *The Quaternary Research* (*Daiyonki-Kenkyu*) 21, 255–271.

Yokoyama, Y., Nakada, M., Maeda, Y., Nagaoka, S., Okuno, J., Matsumoto, E., Sato, H., Matsushima, Y., 1996. Holocene sea-level change and hydro-isostasy along the west coast of Kyushu, Japan. *Palaeogeography, Palaeoclimatology, Palaeoecology* 123, 29–47.

Yokoyama, Y., Okuno, J.I., Miyairi, Y., Obrochta, S., Demboya, N., Makino, Y., Kawahata, H., 2012. Holocene sea-level change and Antarctic melting history derived from geological observations and geophysical modeling along the Shimokita Peninsula, northern Japan. *Geophysical Research Letters* 39, L13502. http://dx.doi.org/10.1029/2012GL051983.

Yonekura, N., 1975. Quaternary tectonic movements in the outer arc of southwest Japan with special reference to seismic crustal deformation. *Bulletin of the Department of Geography, University of Tokyo* 7, 19–71.

Yoshino, K., 1998. Study of shell-mounds in the Middle and Latter Jomon period on Pakeo-Kinu bay by analyzing the composition of shellfish. *Kaizuka-kenkyu* (*The shell mound research*) 3, 15–58.

https://doi.org/10.1017/qua.2019.69 Published online by Cambridge University Press